AD-A096 277 OHIO STATE UNIV COLUMBUS ELECTROSCIENCE LAB F/G 9/5
ANNULAR SLOTS WITH CARDIOID-TYPE PATTERNS.(U)
OCT 80 K AYABE, B A MUNK N00014-78-C-0855
UNCLASSIFIED ESL-711559-1 NL

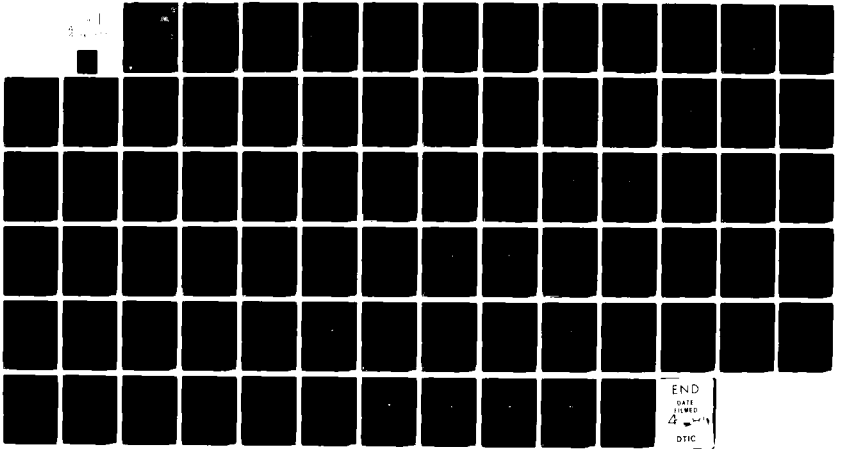

END
DATE FILMED
4-81
DTIC

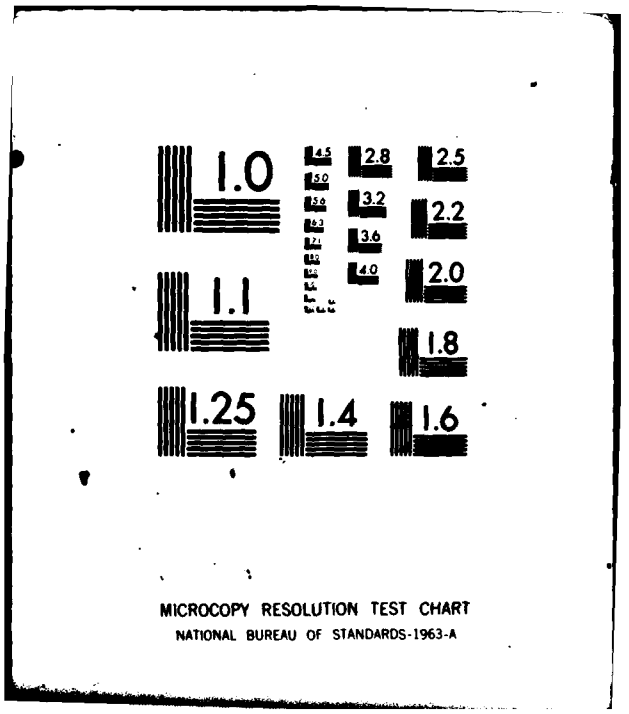
1.0
1.1
1.25
1.4
1.6
1.8
2.0
2.2
2.5
2.8
3.2
3.6
4.0
4.5
5.0
5.6
6.3
7.1
8.0
9.0
10.0
MICROCOPY RESOLUTION TEST CHART
NATIONAL BUREAU OF STANDARDS-1963-A

OSU

The Ohio State University

ANNULAR SLOTS WITH CARDIOID-TYPE PATTERNS

Koichi Ayabe and R. A. Mack

LEVEL II

The Ohio State University

ElectroScience Laboratory

Department of Electrical Engineering
Columbus, Ohio 43212

Technical Report 711559-1

October 1980

Contract N00014-78-C-0855

Department of the Navy
Office of Naval Research
800 North Quincy Street
Arlington, Virginia 22217

Approved for public release;
distribution unlimited

NOTICES

When Government drawings, specifications, or other data are used for any purpose other than in connection with a definitely related Government procurement operation, the United States Government thereby incurs no responsibility nor any obligation whatsoever; and the fact that the Government may have formulated, furnished, or in any way supplied the said drawings, specifications, or other data, is not to be regarded by implication or otherwise as in any manner licensing the holder or any other person or conveying any rights or permission to manufacture, use, or sell any patented invention that may in any way be related thereto.

SECURITY CLASSIFICATION OF THIS PAGE (When Data Entered)

REPORT DOCUMENTATION PAGE

READ INSTRUCTIONS BEFORE COMPLETING FORM

1. REPORT NUMBER

2. GOVT ACCESSION NO. AD-A096277

3. RECIPIENT'S CATALOG NUMBER

4. TITLE (and Subtitle)
Annular Slots with Cardioid-Type Patterns

5. TYPE OF REPORT & PERIOD COVERED
Technical Report

6. PERFORMING ORG. REPORT NUMBER
ESL-711559-1

7. AUTHOR(s)
Koichi Ayabe and B. A. Munk

8. CONTRACT OR GRANT NUMBER(s)
N00014-78-C-0855

9. PERFORMING ORGANIZATION NAME AND ADDRESS
The Ohio State University ElectroScience Laboratory, Department of Electrical Engineering
Columbus, Ohio 43212

10. PROGRAM ELEMENT, PROJECT, TASK AREA & WORK UNIT NUMBERS
Project N00173-78-RQ-0714/7-28-78

11. CONTROLLING OFFICE NAME AND ADDRESS
Department of the Navy
Office of Naval Research, 800 N. Quincy Street
Arlington, Virginia 22217

12. REPORT DATE
October 1980

13. NUMBER OF PAGES
74

14. MONITORING AGENCY NAME & ADDRESS(if different from Controlling Office)

15. SECURITY CLASS. (of this report)
Unclassified

15a. DECLASSIFICATION/DOWNGRADING SCHEDULE

16. DISTRIBUTION STATEMENT (of this Report)

17. DISTRIBUTION STATEMENT (of the abstract entered in Block 20, if different from Report)

18. SUPPLEMENTARY NOTES

19. KEY WORDS (Continue on reverse side if necessary and identify by block number)
Loop antenna
Multiple loop
Multi Mode loop
Cardioid pattern

20. ABSTRACT (Continue on reverse side if necessary and identify by block number)
This report considers the radiation pattern from one or more concentric circular loops. The current on each loop is comprised of components of the form $\sin n\phi$. It is shown how directive patterns with one and more nulls can be obtained in particularly a true cardioid pattern. Particular attention is given to the tolerances in order to maintain a reasonable sharp null.

DD FORM 1 JAN 73 1473 EDITION OF 1 NOV 65 IS OBSOLETE

SECURITY CLASSIFICATION OF THIS PAGE (When Data Entered)

402251

ACKNOWLEDGMENTS

The authors would like to extend their sincere thanks to Mr. Lee W. Henderson for reviewing the manuscript.

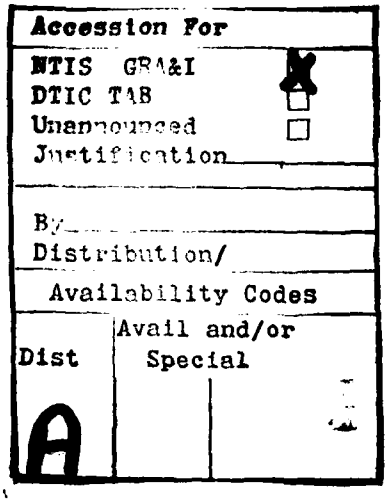

TABLE OF CONTENTS

1. INTRODUCTION

The purpose of this report is to analyze and control the pattern of an annular slot antenna. This antenna is intended to have a null in a horizontal plane over some frequency range. The pattern is, therefore, desired to be a cardioid-type. To realize the cardioid-type pattern, this antenna has multiple-driving points, concentric dual loops or some combination of these. A slot antenna may be analyzed as a magnetic current. In this report, for simplicity, the slot antenna is replaced by a thin wire loop antenna (its compliment) and the analysis is made by using electrical current. For the purpose of the present study this assumption is adequate.

In Sections 2.1 and 2.2 we give a short review of a single wire loop antenna as given by R.W.P. King.[1] The multiple-driven loop antenna is analyzed in Section 2.3. The cardioid condition is next considered in a general way in Section 3. The following sections are devoted to the cardioid condition analysis for various special configuration of antennas when feeding conditions are perturbed. In the last two sections we consider antennas having nulls in three directions

2. RADIATION FROM A LOOP

2.1 Current in a Loop

The configuration of the loop and the coordinate system is shown in Figure 2-1. The center of the loop coincides with the origin of a cylindrical coordinate system and the loop is placed in plane Z=0 (horizontal plane). The radius a of the wire is assumed to be small compared with the radius b of the loop and also small with the wave length. That is,

$$a << b \qquad (2\text{-}1)$$

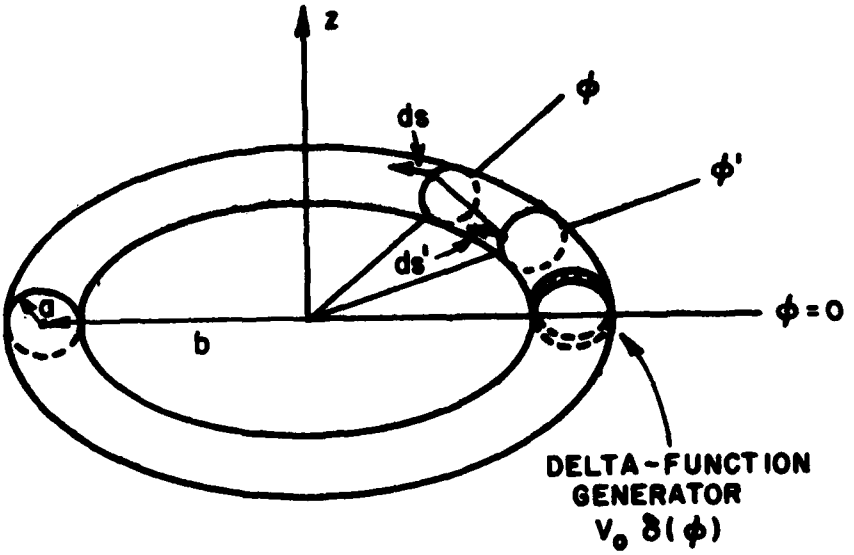

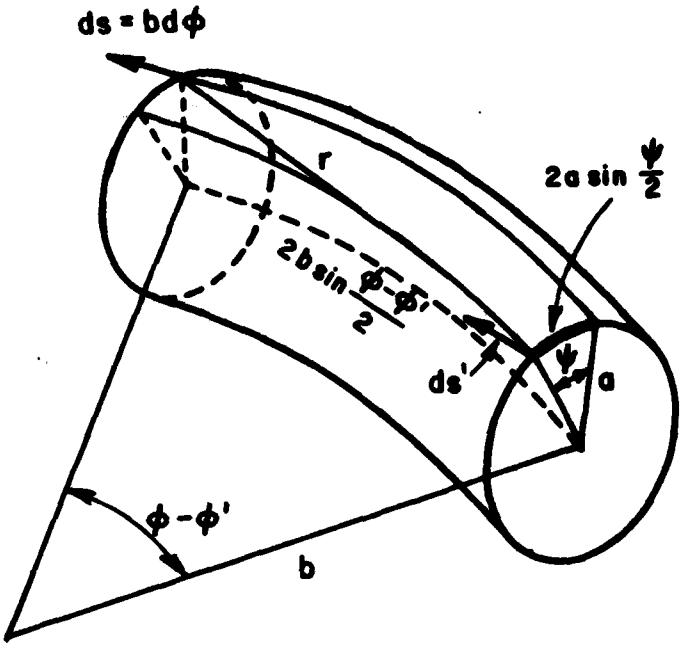

Figure 2-1. General circular loop antenna and coordinate systems.

$$\beta a << 1 \tag{2-2}$$

where $\beta=2\pi/\lambda$ is the propagation constant in free space.

The delta function generator $V_0\delta(\phi)$ is placed at $\phi=0$. The total current in the conductor at ϕ' is $I(\phi')$, and the direction of this element is $ds'=bd\phi'$. The integral equation for $I(\phi')$ is obtained from the boundary condition at the surface of the loop, i.e., the tangential component of the electric field is zero at the surface of the conducting wire. Since

$$\bar{E} = -\nabla V - j\omega\bar{A}, \tag{2-3}$$

$$E_\phi = -V_0\delta(\phi)/b = -\frac{1}{\rho}\frac{\partial V}{\partial \phi} - j\omega A_\phi\Big|_{\rho=b} \quad . \tag{2-4}$$

The scalor and vector potentials at the element $ds=bd\phi$ on the surface of the wire at ϕ are given by[1]:

$$V = \frac{1}{4\pi\varepsilon_0}\int_{\pi}^{\pi} q(\phi')\, w(\phi-\phi')\, d\phi' \tag{2-5}$$

$$A_\phi = \frac{\mu}{4\pi}\int_{\pi}^{\pi} I(\phi')w(\phi-\phi')\cos(\phi-\phi')d\phi' \tag{2-6}$$

where the kernel is

$$w(\phi-\phi') = \frac{b}{2\pi}\int_{-\pi}^{\pi}\frac{e^{-j\beta r}}{r}\, d\psi \tag{2-7}$$

with

$$r = \sqrt{4b^2\sin^2\left[(\phi-\phi')/2\right] + 4a^2\sin^2(\psi/2)} \tag{2-8}$$

The continuity equation for the current and charge in the loop is

$$\frac{dI(\phi')}{bd\phi'} = -j\omega q(\phi') \tag{2-9}$$

From Equations (2-5) and (2-9)

$$\frac{\partial V}{\partial \phi} = \frac{j}{4\pi\varepsilon_0 \omega b} \frac{\partial^2}{\partial \phi^2} \int_{-\pi}^{\pi} I(\phi')w(\phi-\phi')d\phi' \qquad (2\text{-}10)$$

From Equations (2-10), (2-6) and (2-4), the following integral equation is obtained

$$V_0\delta(\phi) = \frac{jZ_0}{4\pi} \int_{-\pi}^{\pi} k(\phi-\phi')I(\phi')d\phi' \qquad (2\text{-}11)$$

where the kernel is

$$k(\phi-\phi') = \left[\beta b\cos(\phi-\phi') + \frac{1}{\beta b} \frac{\partial^2}{\partial \phi^2}\right] w(\phi-\phi') \qquad (2\text{-}12)$$

and

$$Z_0 = \omega\mu/\beta = \sqrt{\mu/\varepsilon_0} \quad . \qquad (2\text{-}13)$$

A solution of the integral equation (2-11) may be sought with the aid of the Fourier expansion of the kernel and of the current. The dimensionless quality $w(\phi-\phi')$ is expanded as

$$w(\phi-\phi') = \sum_{-\infty}^{\infty} k_m e^{-jm(\phi-\phi')} \qquad (2\text{-}14)$$

where

$$k_m = \frac{1}{2\pi} \int_{-\pi}^{\pi} w(\phi-\phi')e^{jm(\phi-\phi')} d\phi' = k_{-m} \qquad (2\text{-}15)$$

Equations (2-14) and (2-15) are substituted into Equation (2-12)

$$k(\phi-\phi') = \sum_{-\infty}^{\infty} \alpha_n e^{-jn(\phi-\phi')} \qquad (2\text{-}16)$$

where

$$\alpha_n = \frac{\beta b}{2}(k_{n+1} + k_{n-1}) - \frac{n^2}{\beta b} \quad k_n = -\alpha_{-n} \tag{2-17}$$

Now the integral equation is reduced to

$$V_0\delta(\phi) = \frac{jZ_0}{4\pi} \sum_{-\infty}^{\infty} \alpha_n \int_{-\pi}^{\pi} e^{-jn(\phi-\phi')} I(\phi')d\phi' \tag{2-18}$$

The current $I(\phi')$ is also expanded in a Fourier series

$$I(\phi') = \sum_{-\infty}^{\infty} I_n e^{-jn\phi} \tag{2-19}$$

where

$$I_n = \frac{1}{2\pi} \int_{-\pi}^{\pi} I(\phi') e^{jn\phi'} \, d\phi' \tag{2-20}$$

A comparison of Equations (2-18) and (2-20) shows that

$$v_0\delta(\phi) = \frac{jZ_0}{2} \sum_{-\infty}^{\infty} \alpha_n \, I_n \, e^{-jn\phi} \tag{2-21}$$

This is a Fourier series with the coefficient $(jZ_0/2)\,\alpha_n I_n$. The coefficients are given by

$$j\frac{Z_0}{2}\alpha_n \, I_n = \frac{1}{2\pi} \int_{-\pi}^{\pi} V_0\delta(\phi) e^{jn\phi} \, d\phi = \frac{V_0}{2\pi} \tag{2-22}$$

Thus

$$I_n = -\frac{jV_0}{Z_0\pi\alpha_n} \tag{2-23}$$

so that

$$I(\phi) = \sum_{-\infty}^{\infty} I_n e^{-jn\phi} = -\frac{jV_0}{Z_0\pi}\left(\frac{1}{\alpha_0} + 2\sum_{1}^{\infty} \frac{\cos n\phi}{\alpha_n}\right) \tag{2-24}$$

The coefficient α_n can be calculated by Equation (2-17) with the following equations and its results are shown in Figure 2-2.

$$k_0 = \frac{1}{\pi} \ln \frac{8b}{a} - \frac{1}{2}\left[\int_0^{2\beta b} \Omega_0(x)dx + j\int_0^{2\beta b} J_0(x)dx\right] \qquad (2\text{-}25)$$

$$k_{-n}=k_n = \frac{1}{\pi}\left[K_0(\frac{na}{b})I_0(\frac{na}{b}) + C_n\right] - \frac{1}{2}\int_0^{2\beta b}\left[\Omega_{2n}(x)+jJ_{2n}(x)\ dx\right] \qquad (2\text{-}26)$$

where

$I_0(\frac{na}{b})$ is the modified Bessel function of the first kind

$K_0(\frac{na}{b})$ is the modified Bessel function of the second kind

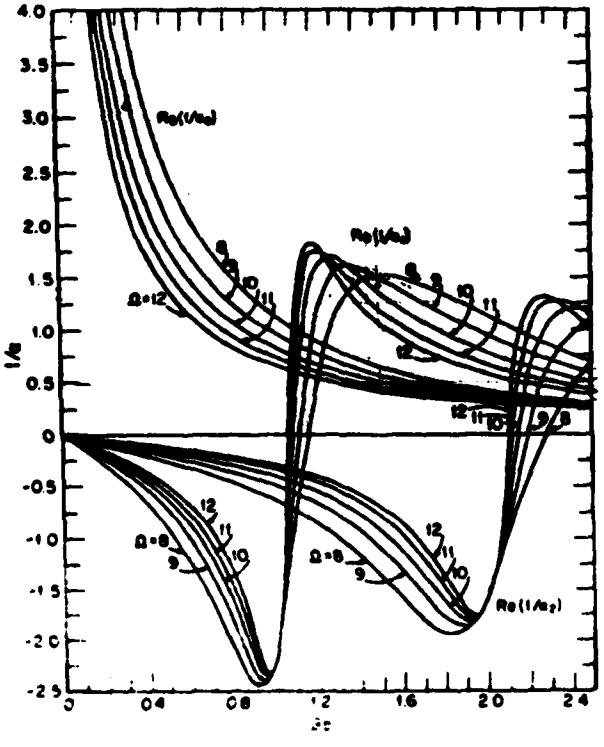

Figure 2-2(a). Real parts of the coefficients $1/\alpha_0$, $1/\alpha_1$, $1/\alpha_2$.

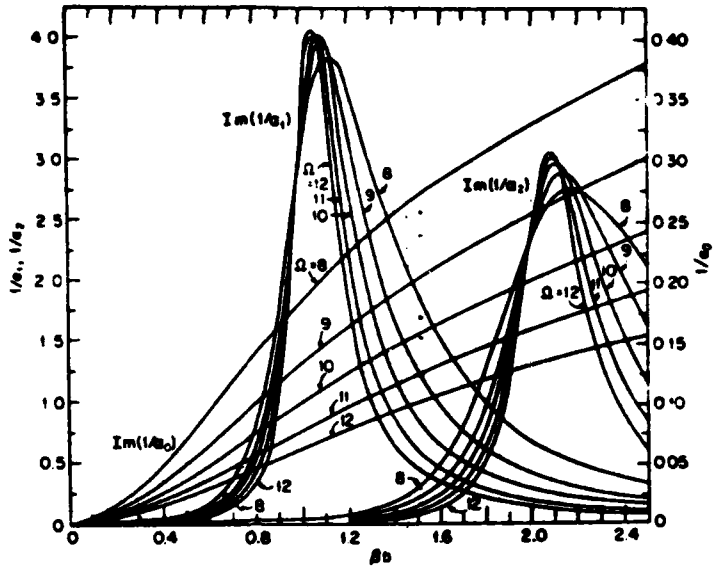

Figure 2-2(b) Imaginary parts of the coefficients $1/\alpha_0$, $1/\alpha_1$, $1/\alpha_2$.

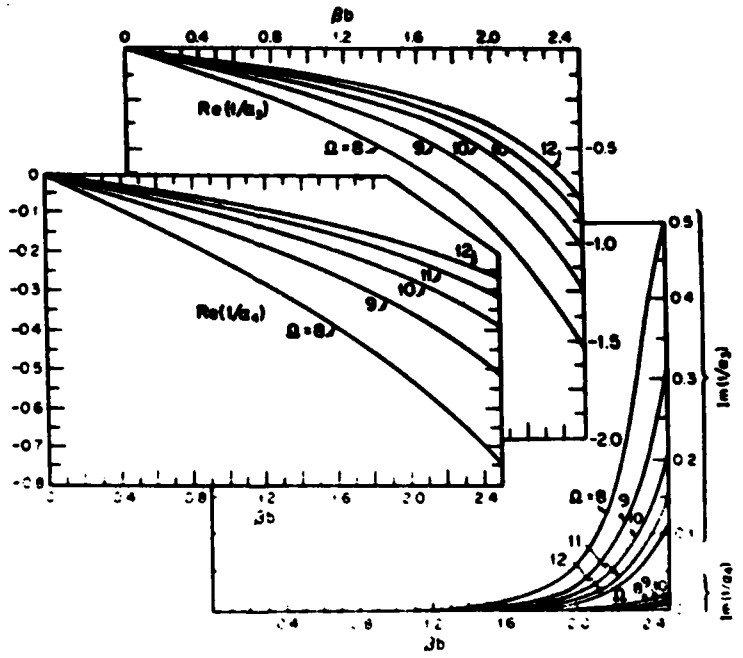

Figure 2-2(c). Real and imaginary parts of the coefficients $1/\alpha_3$ and $1/\alpha_4$.

$$C_n = \ln 4n + \gamma - 2 \sum_{m=0}^{n-1} \frac{1}{2m+1}$$

γ is 0.57721 (Eulers number)

$J_n(x)$ is the Bessel function of first kind of order n

$\Omega_n(x)$ is the Lommel-Weber function of order n

2.2 Radiation From the Loop

The coordinate system and the loop are shown in Figure 2-3. The center of the loop coincides with the origin of the coordinate system. Current distribution is given by Equation (2-24)

$$I(\phi) = -\frac{jV_0}{\pi Z_0} \sum_{-\infty}^{\infty} \frac{e^{jn\phi}}{\alpha_n} \qquad (2\text{-}27)$$

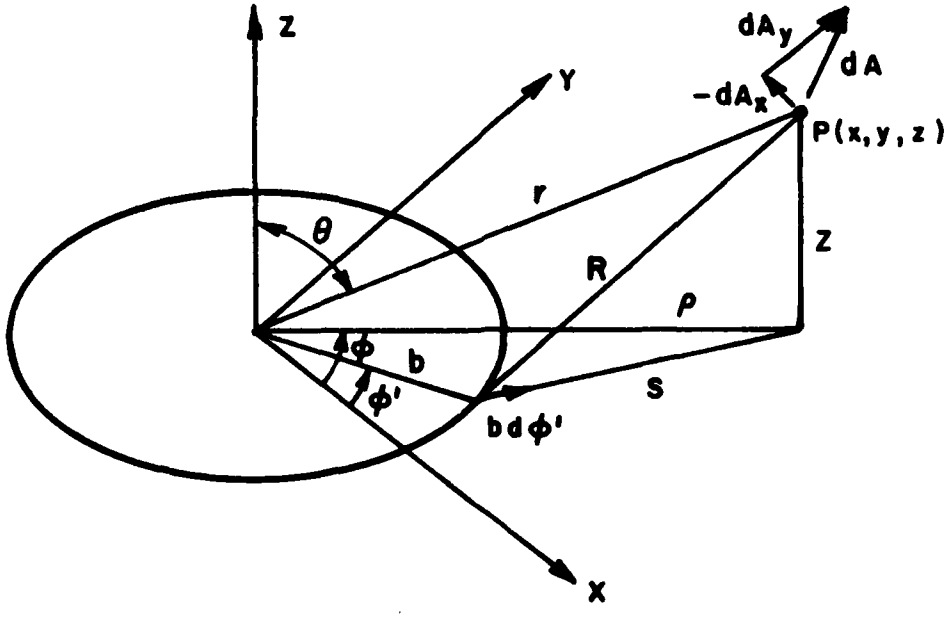

Figure 2-3. Loop antenna and coordinate system for radiation calculation.

Vector potential $d\bar{A}$ at the point P(x,y,z) or (r,θ,ϕ) due to the current in the element $bd\phi'$ is

$$d\bar{A} = \hat{\phi}\,\frac{\mu}{4\pi}\,\frac{e^{-j\beta R}}{R}\,I(\phi')bd\phi' \tag{2-28}$$

where

$$\begin{aligned} R &= \sqrt{Z^2+S^2} \\ &= \sqrt{(r\cos\theta)^2 + \rho^2+b^2-2\rho b\cos(\phi-\phi')} \\ &\approx r-b\sin\theta\cos(\phi-\phi') \end{aligned} \tag{2-29}$$

For the far field we have

$$b \ll r \tag{2-30}$$

and the x and y components of the vector potential at point P are then obtained from the following integrals

$$\begin{aligned} A_x &= -\int_0^{2\pi} \sin\phi'\, dA \\ &= -\frac{b\mu}{4\pi}\,\frac{e^{-j\beta r}}{r}\int_0^{2\pi} I(\phi')\, e^{j\beta b\sin\theta\cos(\phi-\phi')}\,\sin\phi' d\phi' \end{aligned} \tag{2-31}$$

$$\begin{aligned} A_y &= \int_0^{2\pi} \cos\phi'\, dA \\ &= \frac{b\mu}{4\pi}\,\frac{e^{-j\beta r}}{r}\int_0^{2\pi} I(\phi')\, e^{j\beta b\sin\theta\cos(\phi-\phi')}\,\cos\phi' d\phi' \end{aligned} \tag{2-32}$$

Equation (2-27) is inserted into Equations (2-31) and (2-32), and $\sin\phi$ and $\cos\phi$ are expressed in exponential form. The n^{th} component of A_x and A_y are expressed as follows

$$A_{xn} = \frac{Q_n}{j2} (-k_1+k_2) \tag{2-33}$$

$$A_{yn} = \frac{Q_n}{2} (k_1+k_2) \tag{2-34}$$

where

$$Q_n = \frac{-jb_\mu e^{-j\beta r} V_o}{4\pi^2 r Z_o \alpha_n} \tag{2-35}$$

$$k_1 = \int_0^{2\pi} e^{j(n+1)\phi'} e^{jB\cos(\phi-\phi')} d\phi' \tag{2-36}$$

$$k_2 = \int_0^{2\pi} e^{j(n-1)\phi'} e^{jB\cos(\phi-\phi')} d\phi' \tag{2-37}$$

$$B = \beta b \sin\theta \tag{2-38}$$

k_1 and k_2 are very similar to the Sommerfeld representation of Bessel function :

$$J_n(B) = \frac{j^{-n}}{2\pi} \int_0^{2\pi} e^{jB\cos\phi} e^{jn\phi} d\phi \tag{2-39}$$

Inspection of Equations (2-36) through (2-39) shows that k_1 and k_2 can be expressed as

$$k_1 = 2\pi j^{n+1} e^{j(n+1)\phi} J_{n+1}(B) \tag{2-40}$$

$$k_2 = 2\pi j^{n-1} e^{j(n-1)\phi} J_{n-1}(B) \tag{2-41}$$

The spherical components of the vector potential due to the current component $I_n(\phi)$ are

$$A_{\theta n} = (A_{xn}\cos\phi + A_{yn}\sin\phi)\cos\theta \tag{2-42}$$

$$A_{\phi n} = (-A_{xn}\sin\phi + A_{yn}\cos\phi) \tag{2-43}$$

The resultant vector potential is the sum of each component:

$$A_\theta = \sum_{-\infty}^{\infty} A_{\theta n}$$

$$= -2\pi \sum_{-\infty}^{\infty} Q_n e^{jn(\phi+\pi/2)} \frac{n}{B} J_n(B)\cos\theta \tag{2-44}$$

$$A_\phi = \sum_{-\infty}^{\infty} A_{\phi n}$$

$$= -j2\pi \sum_{-\infty}^{\infty} Q_n e^{jn(\phi+\pi/2)} J_n'(B) \tag{2-45}$$

Substituting Equations (2-35) and (2-38) into Equations (2-44) and (2-45) yields

$$A_\theta = Q V_o b \sum_{-\infty}^{\infty} \frac{n e^{jn(\phi+\pi/2)} J_n(\beta b\sin\theta)\cos\theta}{\alpha_n \beta b\sin\theta} \tag{2-46}$$

$$A_\phi = jQV_o b \sum_{-\infty}^{\infty} \frac{e^{jn(\phi+\pi/2)}}{\alpha_n} J_n'(\beta b\sin\theta) \tag{2-47}$$

where

$$Q = \frac{j\mu e^{-j\beta r}}{2\pi Z_o r} \tag{2-48}$$

Alternately

$$A_\theta = Q\, V_o b \sum_1^\infty \frac{n}{\alpha_n} \frac{J_n(\beta b \sin\theta)}{\beta b \sin\theta} \cos\theta$$

$$\times \left[e^{jn(\phi+\pi/2)} - (-1)^n e^{-jn(\phi+\pi/2)} \right] \qquad (2\text{-}49)$$

$$A_\phi = jQ\, V_o\, b \left\{ \frac{J_o'(\beta b \sin\theta)}{\alpha_o} \right.$$

$$\left. + \sum_1^\infty \frac{J_n'(\beta b \sin\theta)}{\alpha_n} \left[e^{jn(\phi+\pi/2)} + (-1) e^{-jn(\phi+\pi/2)} \right] \right\} \qquad (2\text{-}50)$$

For loops of moderate size, $\beta b < 2.5$, the principal contribution to the current are from the first three terms in the series. The vector potentials are

$$A_\theta = QV_o b \left[0 - \frac{2J_1(\beta b \sin\theta)\cos\theta \sin\phi}{\alpha_1\, \beta b \sin\theta} - \frac{j4J_2(\beta b \sin\theta)\cos\theta \sin 2\phi}{\alpha_2\, \beta b \sin\theta} \right] \qquad (2\text{-}51)$$

$$A_\phi = jQV_o b \left[\frac{J_o'(\beta b \sin\theta)}{\alpha_o} + \frac{j2J_1'(\beta b \sin\theta)\cos\phi}{\alpha_1} - \frac{2J_2'(\beta b \sin\theta)\cos 2\phi}{\alpha_2} \right] \qquad (2\text{-}52)$$

The electromagnetic field is given by

$$\bar{E} = j\omega\hat{r}x(\hat{r}x\bar{A}) = - j\omega(\hat{\theta}A_\theta+\hat{\phi}A_\phi) \tag{2-53}$$

$$\bar{B} = - j\beta\hat{r}x\bar{A} = - j\beta(\hat{\phi}A_\theta-\hat{\theta}A_\phi) \tag{2-54}$$

Therefore

$$E_\theta = j\omega QV_o b\left[\frac{2J_1(\beta b\sin\theta)\cos\theta\sin\phi}{\alpha_1\beta b\sin\theta} - j\,\frac{4J_2(\beta b\sin\theta)\cos\theta\sin 2\phi}{\alpha_2\beta b\sin\theta}\right] \tag{2-55}$$

$$E_\phi = \omega QV_o b\left[\frac{J_o'(\beta b\sin\theta)}{\alpha_o} + j\,\frac{2J_1'(\beta b\sin\theta)\cos\phi}{\alpha_1} - \frac{2J_2'(\beta b\sin\theta)\cos 2\phi}{\alpha_2}\right] \tag{2-56}$$

2.3 Multiply-driven Loop

The current and vector potentials in the loop which is driven by the generator V_a at $\phi=0$ are obtained from Equations (2-24), (2-46) and (2-47), respectively:

$$I_a(\phi) = - \frac{jV_a}{\pi Z_o}\sum_{-\infty}^{\infty}\frac{e^{jn\phi}}{\alpha_n} \tag{2-57}$$

$$A_{\theta_a} = QV_a b\sum_{-\infty}^{\infty}\frac{ne^{jn(\phi+\pi/2)}\,J_n(\beta b\sin\theta)\cos\theta}{\alpha_n\,\beta b\sin\theta} \tag{2-58}$$

$$A_{\phi a} = jQV_a b \sum_{-\infty}^{\infty} \frac{e^{jn(\phi+\pi/2)} J_n'(\beta b \sin\theta)}{\alpha_n} \tag{2-59}$$

If generator position is changed from $\phi=0$ to $\phi=\phi_b$, and voltage from V_a to V_b, the current and vector potentials are given by

$$I_b(\phi) = -\frac{jV_b}{\pi Z_o} \sum_{-\infty}^{\infty} \frac{e^{jn(\phi-\phi_b)}}{\alpha_n} \tag{2-60}$$

$$A_{\theta b} = QV_b b \sum_{-\infty}^{\infty} \frac{n\, e^{jn(\phi-\phi_b+\pi/2)} J_n(\beta b \sin\theta)\cos\theta}{\alpha_n\, \beta b \sin\theta} \tag{2-61}$$

$$A_{\phi b} = jQV_b\, b \sum_{-\infty}^{\infty} \frac{e^{jn(\phi-\phi_b+\pi/2)} J_n'(\beta b \sin\theta)}{\alpha_n} \tag{2-62}$$

If the loop is driven by two generators shown in Figure 2-4, the current in the loop is expressed as the sum of $I_a(\phi)$ and $I_b(\phi)$.

$$I(\phi) = I_a(\phi) + I_b(\phi)$$

$$= -j\frac{V_a}{\pi Z_o} \sum_{-\infty}^{\infty} \frac{e^{jn\phi}}{\alpha_n} - j\frac{V_b}{\pi Z_o} \sum_{-\infty}^{\infty} \frac{e^{jn(\phi-\phi_b)}}{\alpha_n} \tag{2-63}$$

The vector potentials are also the sum of each vector potentials.

$$A_\theta = A_{\theta a} + A_{\theta b}$$

$$= Qb \sum_{-\infty}^{\infty} \frac{nJ_n(\beta b \sin\theta)\cos\theta}{\alpha_n\, \beta b \sin\theta} \left[V_a\, e^{jn(\phi+\pi/2)} + V_b e^{jn(\phi-\phi_b+\pi/2)} \right] \tag{2-64}$$

$$A_\phi = A_{\phi a} + A_{\phi b}$$

$$= jQb \sum_{-\infty}^{\infty} \frac{J_n'(\beta b \sin\theta)}{\alpha_n} \left[V_a e^{jn(\phi+\pi/2)} + V_b e^{jn(\phi-\phi_b+\pi/2)} \right] \tag{2-65}$$

As a special case, the loop is assumed to have two generators at $\phi=0$ and $\phi=\pi$, and the voltages V_a and V_b, are as shown in Figure 2-5. Substituting $\phi_b=\pi$ in Equations (2-64) and (2-65), the following equations are obtained:

$$A_\theta = Qb \sum_{-\infty}^{\infty} \frac{nJ_n(\beta b \sin\theta)\cos\theta}{\alpha_n \beta b \sin\theta} \left[V_a e^{jn(\phi+\pi/2)} + V_b e^{jn(\phi-\pi/2)} \right] \tag{2-66}$$

$$A_\phi = jQb \sum_{-\infty}^{\infty} \frac{J_n'(\beta b \sin\theta)}{\alpha_n} \left[V_a e^{jn(\phi+\pi/2)} + V_b e^{jn(\phi-\pi/2)} \right] \tag{2-67}$$

If n is limited to 0 and 1, the electromagnetic field is expressed as follows:

$$E_\theta = \frac{j\, 2\omega\, Qb J_1(\beta b \sin\theta)\cos\theta \cos\phi}{\alpha_1 \beta b \sin\theta} (V_a - V_b) \tag{2-68}$$

$$E_\phi = \frac{\omega Qb\, J_0'(\beta b \sin\theta)(V_a+V_b)}{\alpha_0} + \frac{j2\omega\, Qb J_1'(\beta b \sin\theta)(V_a-V_b)\cos\phi}{\alpha_1} \tag{2-69}$$

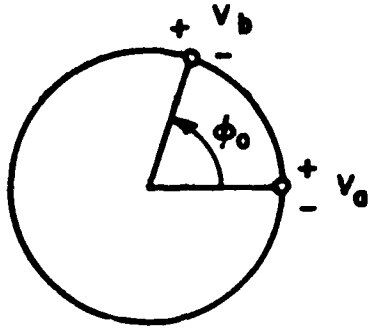

Figure 2-4. General multiple-driven loop antenna.

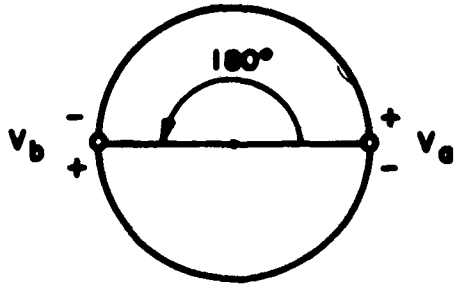

Figure 2-5. Loop antenna driven at two points.

3. CONDITION FOR CARDIOID PATTERN

Both in the singly driven (2-24) or multiple driven (2-62) loop, the current in the loop is expressed as follows

$$I(\phi) = \sum_{-\infty}^{\infty} (C_n e^{jn\phi})$$

$$= C_o + \sum_{n=1}^{\infty} 2C_n \cos n\phi \qquad (3\text{-}1)$$

where $C_n = C_{-n}$ is a complex constant which is determined by many factors such as frequency, physical size of the loop, configuration of drive (one point, two points or four points) or voltage applied to each terminal. Consequently the electric field is unitarily expressed as

$$E = \sum_{-\infty}^{\infty} E_n e^{jn\phi}$$

$$= E_o + \sum_{n=1}^{\infty} 2E_n \cos n\phi \qquad (3\text{-}2)$$

This means that the resultant electromagnetic field is the sum of each mode of field components. Now let us consider the electric field in the plane of $\theta=90^o$ and mode is limited to n=0 and n=1. From Equations (2-55) and (2-56)

$$E_\theta = 0 \qquad (3\text{-}3)$$

$$E_\phi = E_{\phi o} + E_{\phi 1} \cos\phi \qquad (3\text{-}4)$$

where

$$E_{\phi o} = \frac{\omega \eta V_o h J_o'(\beta b)}{\alpha_o} \qquad (3\text{-}5)$$

$$E_{\phi 1} = \frac{j2\omega Q V_0 b J_1'(\beta b)}{\alpha_1} \tag{3-6}$$

If $E_{\phi 0} = E_{\phi 1}$, (3-7)

Equation (3-4) is reduced to

$$E_\phi = E_{\phi 0}(1+\cos\phi) \quad . \tag{3-8}$$

This is the cardioid pattern shown in Figure 3-1 which has a null at $\phi=180^0$. The cardioid pattern is produced when the peak magnitudes of the n=0 mode (nondirectional pattern in Figure 3-1) and the n=1 mode (Figure eight pattern also in Figure 3-1) are equal. To obtain the cardioid pattern we must control $E_{\phi 0}$ and $E_{\phi 1}$ to satisfy (3-7). The coefficients $E_{\phi 0}$ and $E_{\phi 1}$ are functions of frequency, size of the loop, mode of driving (one point, two points, or four points) or voltage applied to each driving point. These are the parameters to obtain the cardioid pattern. How to select these items are discussed in the following sections. However, it is better to predict how the pattern will change when the cardioid condition is shifted from its optimum value. To this end we rewrite Equation (3-4) as follows:

$$E_\phi = E_{\phi 0}\left[1+(a+jb)\cos\phi\right] \tag{3-9}$$

where a and b are real numbers. The power pattern is expressed as

$$E_\phi^2 = E_{\phi 0}^2\left[(a+b)^2\left(\cos\phi + \frac{a}{a^2+b^2}\right)^2 + \frac{b^2}{a^2+b^2}\right] \tag{3-10}$$

If conversions between E_ϕ^2 and y and between $\cos\phi$ and x are made, Equation (3-10) represents a parabolic curve. From this parabolic curve and circle of unit radius, polar plot of Equation (3-10) can be obtained.

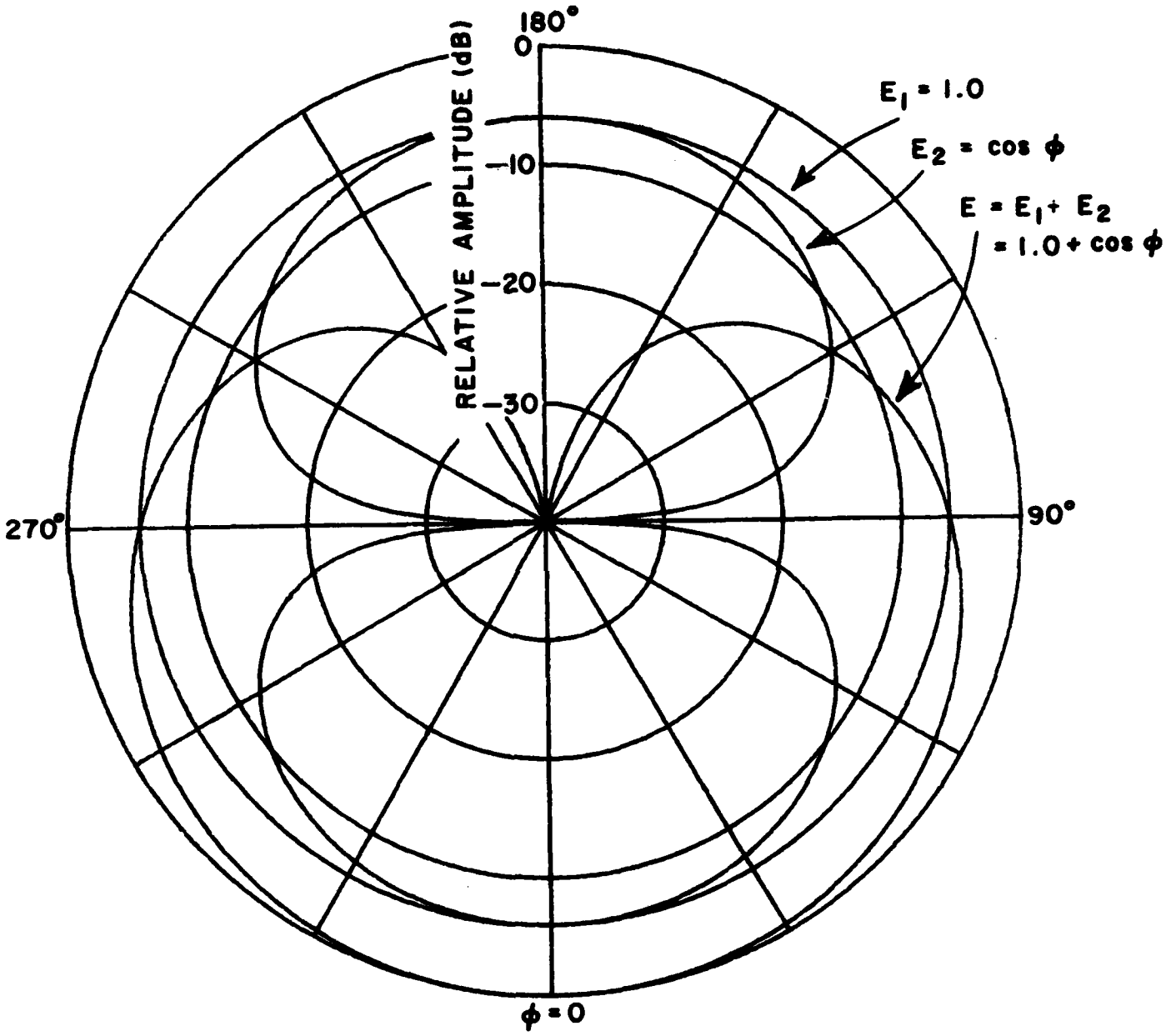

Figure 3-1. Synthesis of cardioid pattern.

In Figure 3-2 we have plotted the parabolic curve. Draw the $\phi=\phi_1$ line from the center of the circle. At the intersection point with the circle a straight line is drawn up to the parabolic curve. The intersection point with the x axis is $\cos\phi_1$. Next, mark the value E_1 on the line in circle and the polar plot is obtained.

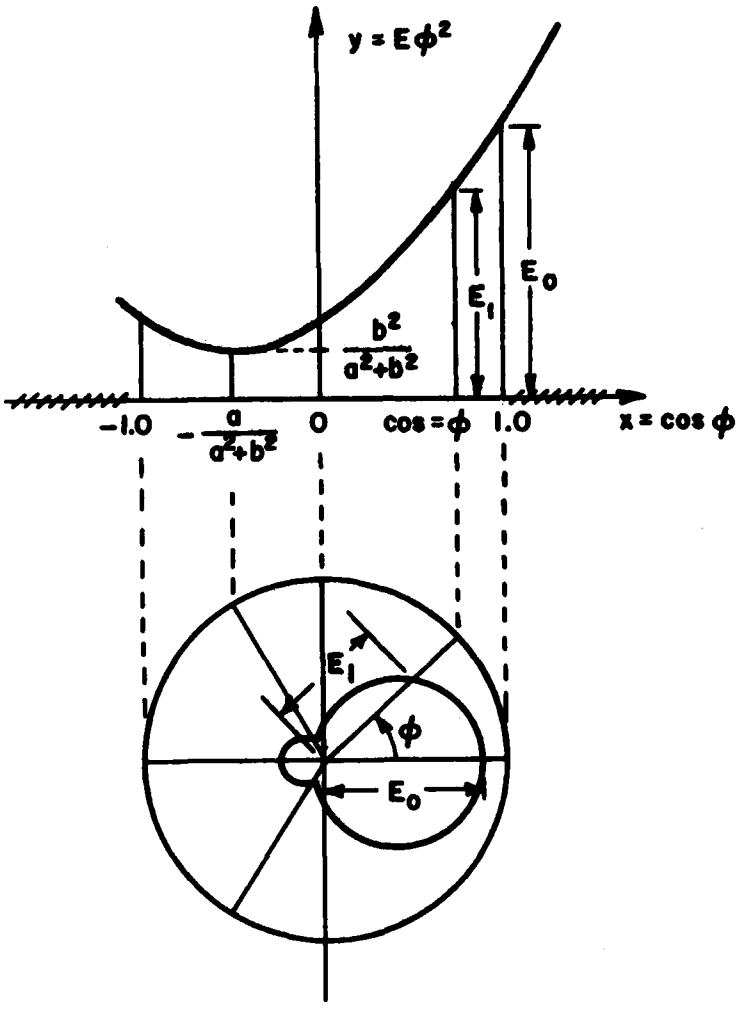

Figure 3-2. How to make a polar plot.

Consider the case shown in Figure 3-2. E_ϕ^2 is maximum at $\phi=0$. As ϕ increases, E_ϕ^2 decreases monotonically. At $\phi=\cos^{-1}(\frac{a}{a^2+b^2})$ E_ϕ^2 yields the minimum $\frac{E^2}{a^2+b^2}$. And again E_ϕ^2 increases to the peak at $\phi=180^0$. The pattern is symmetrical with respect to the $\phi=0$ and 180^0 axis. According to the position of the parabolic curve minimum, the pattern is classified into three types. These are shown in Figure 3-3. Type I (Figure 3-3(a)) is already stated in Figure 3-2, which has two minimum located symmetrically.

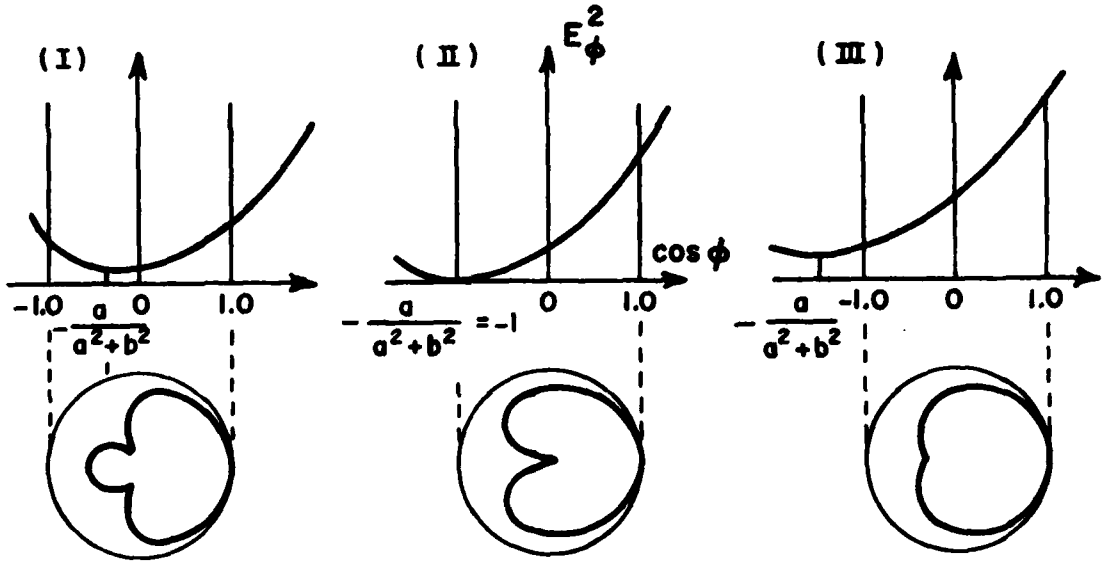

(a) TWO NULLS (b) TRUE CARDIOID (c) ONE NULL

Figure 3-3. Three types of loop antenna pattern in horizontal plane.

This occurs when $-1 < -\frac{a}{a^2+b^2} \leq 0$ $(0>a)$, or $0 \leq -\frac{a}{a^2+b^2} < 1$ $(a<0)$. The region which satisfies this relationship is outside the two circles $(a \pm \frac{1}{2})^2 + b^2 = (\frac{1}{2})^2$ in Figure 3-4. Type II (Figure 3-3(b)) is a special case in which $\cos\phi = -\frac{a}{a^2+b^2} = \pm 1$ and $\frac{b^2}{a^2+b^2} = 0$ that is $a = \pm 1$ and $b = 0$. This is the case when the pattern shows the true cardioid $1 + \cos\phi$.

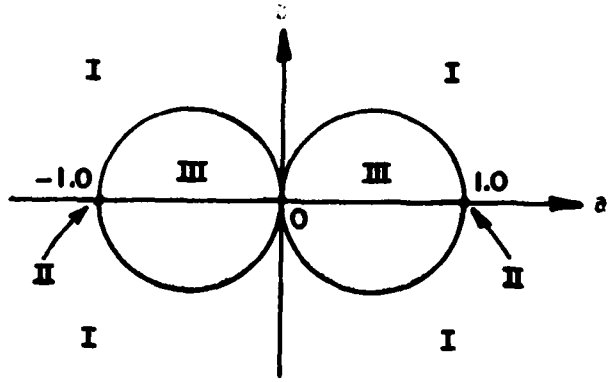

REGION I PRODUCES TWO NULLS
REGION II PRODUCES TRUE CARDIOID
REGION III PRODUCES ONE NULL

Figure 3-4. Region which produces three different patterns in $E=1+(a+jb)\cos\phi$.

Type III (Figure 3-3(c)) occurs when $-\frac{a}{a^2+b^2} < -1$ $(a>0)$ or $1 < -\frac{a}{a^2+b^2}$ $(a<0)$. In this case maximum is at $\phi=0$ $(a>0)$ or $\phi=180^0$ $(a<0)$ and minimum is at $\phi=180^0$ $(a>0)$ or 0^0 $(a<0)$. This pattern resembles Type II except the null is not as deep. The region of a and b is within the circle in Figure 3-4.

4. SINGLE LOOP DRIVEN AT SINGLE POINT

The configuration of this antenna is the same as shown in Figure 2-1. The electric field in the horizontal plane is obtained by substituting $\theta=\pi/2$ into Equations (2-55) and (2-56). If the number of modes is limited to n=0 and n=1. we obtain:

$$E_\theta = 0 \tag{4-1}$$

$$E_\phi = \omega Q V_o b \left[\frac{J_o'(\beta b)}{\alpha_o} + j\,\frac{2J_1'(\beta b)}{\alpha_1}\cos\phi\right] \tag{4-2}$$

If

$$\frac{J_0'(\beta b)}{\alpha_0} = j\frac{2J_1'(\beta b)}{\alpha_1}, \qquad (4\text{-}3)$$

then the cardioid condition (Equation (3-7)) is satisfied. Equation (4-2) is reduced to the type of Equation (3-8). α_0 and α_1 is a function of frequency, the wire radius a and the loop radius b as defined by Equation (2-17).

If a and b are chosen to satisfy Equation (4-3) at a certain frequency, the cardioid pattern is realized. This type of antenna is very simple and desirable. However, only a narrow frequency band satisfies Equation (4-3). Therefore, further investigation of this antenna was not pursued.

5. SINGLE LOOP DRIVEN AT TWO POINTS

5.1 Antenna patterns

The configuration of this type of antenna is shown in Figure 5-1. Two-point-drive means that the pattern is not only restricted by the physical size of the loop, but also controlled by the relative voltage applied to the driving points. The electric field in the horizontal plane is obtained from Equations (2-68) and (2-69):

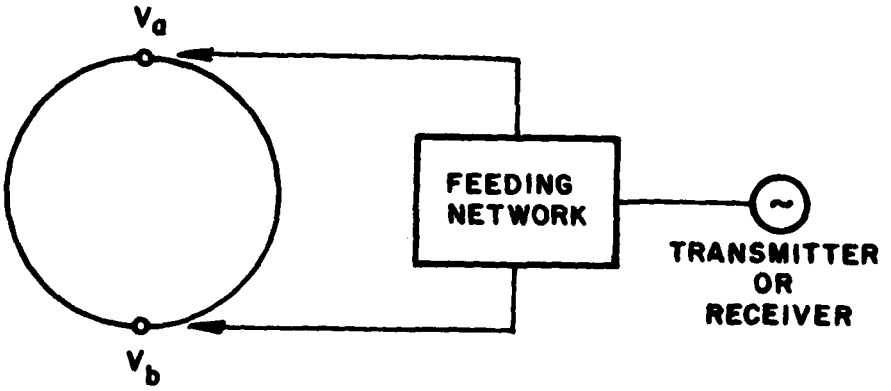

Figure 5-1. Loop antenna fed at two points.

$$E = 0 \tag{5-1}$$

$$E_\phi = Q\omega b \left[\frac{J_0'(\beta b)(V_a+V_b)}{\alpha_0} + j \frac{2J_1'(\beta b)(V_a-V_b)}{\alpha_1} \cos\phi \right] . \tag{5-2}$$

The cardioid condition of a null at $\phi=180^o$ is according to Equation (3-7),

$$\frac{J_0'(\beta b)}{\alpha_0} (V_a+V_b) = j \frac{2J_1'(\beta b)}{\alpha_1} (V_a-V_b) \tag{5-3}$$

Under this condition, Equation (5-2) is reduced to

$$E_\phi(\pi/2,\phi) = \frac{Q\omega b\, J_0'(\beta b)(V_a+V_b)}{\alpha_0} \left[1 + \cos\phi\right] . \tag{5-4}$$

In order to satisfy Equation (5-3) one might select both the physical size (a and b) and the voltages (V_a and V_b). However once the physical size is determined, V_a and V_b must satisfy the following relationship as obtained from Equation (5-3):

$$\frac{V_b}{V_a} = \frac{j\,2\,\frac{\alpha_0}{\alpha_1}\frac{J_1'(\beta b)}{J_0'(\beta b)} - 1}{j\,2\,\frac{\alpha_0}{\alpha_1}\frac{J_1'(\beta b)}{J_0'(\beta b)} + 1} \tag{5-5}$$

Substituting condition (5-5) into Equations (2-66) and (2-67) yields

$$E_\theta(\theta,\phi) = j \frac{2\omega Q}{\alpha_1 \beta} V_a \left(1 - \frac{V_b}{V_a}\right) \frac{J_1(\beta b \sin\theta)\cos\theta}{\sin\theta} \cos\phi \tag{5-6}$$

$$E(\theta,\phi) = \frac{Q\omega b J_0'(\beta b\sin\theta)}{\alpha_0} V_a\left(1+\frac{V_b}{V_a}\right)\left[1 + j2\,\frac{\alpha_0}{\alpha_1}\,\frac{J_1'(\beta b\sin\theta)}{J_0'(\beta b\sin\theta)} \times \frac{1-\frac{V_b}{V_a}}{1+\frac{V_b}{V_a}}\cos\phi\right] \tag{5-7}$$

The patterns in the vertical planes $\phi=0$ and 90^0 are shown in Figures 5-2 and 5-3, respectively. Note that as b increases, energy is radiated more in the vertical direction, and the undesired null is produced as shown in Figure 5-2(b). The pattern of the horizontal plane remains unchanged when βb is changed as seen by inspection of Equation(5-4). If the null direction is desired to be different from $\phi=\pi$, its condition is obtained by substituting $E(\pi/2,\phi_0)=0$ where ϕ_0 is the desired direction of the null. That is

$$\frac{J_0'(\beta b)}{\alpha_0}(V_a+V_b) - j\,\frac{2\,J_1'(\beta b)(V_a-V_b)}{\alpha_1}\cos\phi_0=0 \tag{5-8}$$

or

$$\frac{V_b}{V_a} = \frac{j\,\frac{2\alpha_0}{\alpha_1}\,\frac{J_1'(\beta b)}{J_0'(\beta b)}\cos\phi_0-1}{j\,\frac{2\alpha_0}{\alpha_1}\,\frac{J_1'(\beta b)}{J_0'(\beta b)}\cos\phi_0+1} \tag{5-9}$$

The pattern in the horizontal plane is

$$E_\phi(\pi/2,\phi) = \frac{Q\omega b J_0'(\beta b)(V_a+V_b)}{\alpha_0}\left[1-\frac{1}{\cos\phi_0}\cos\phi\right] \tag{5-10}$$

An example of this pattern is shown in Figure 5-4.

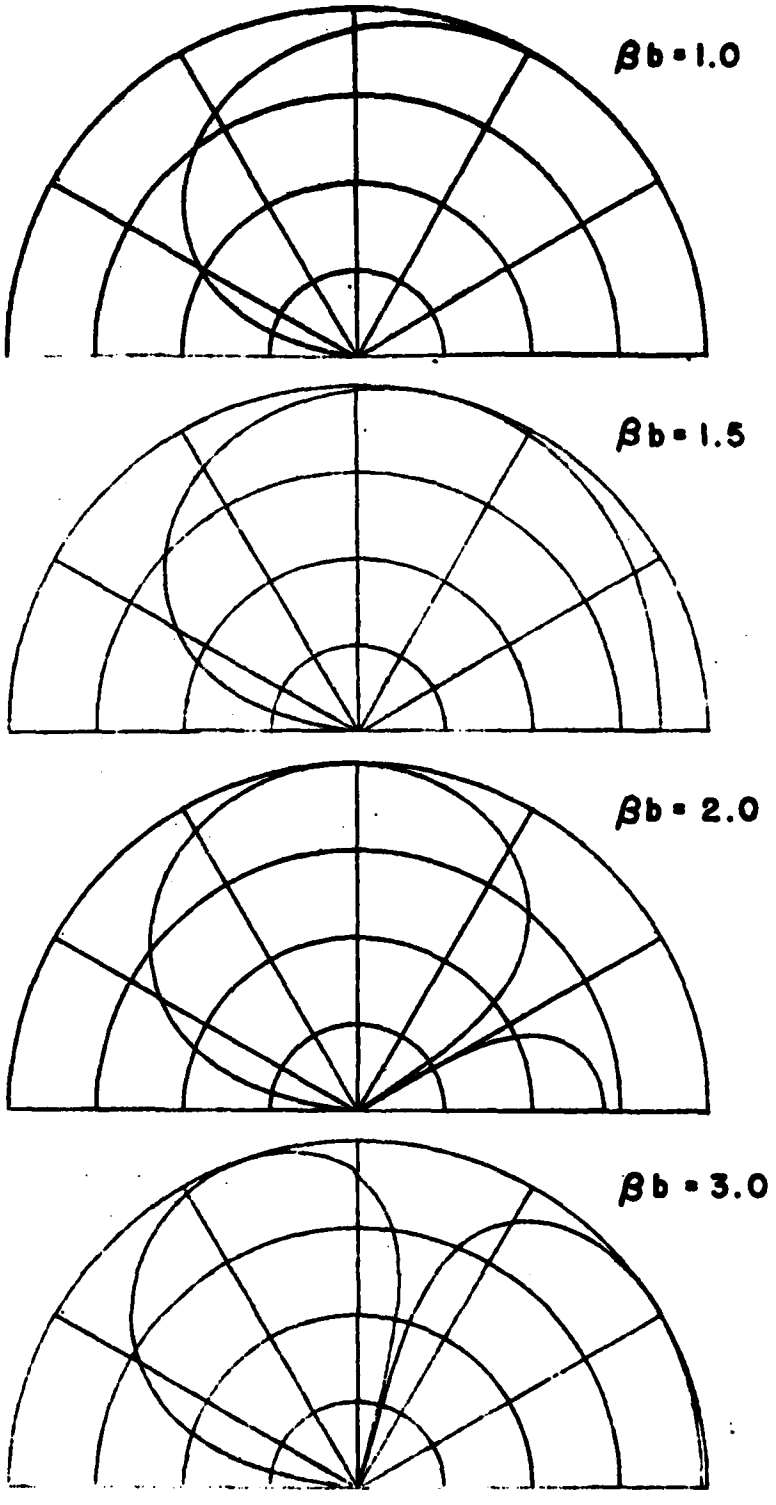

Figure 5-2. Vertical pattern at $\phi=0^{o}$.

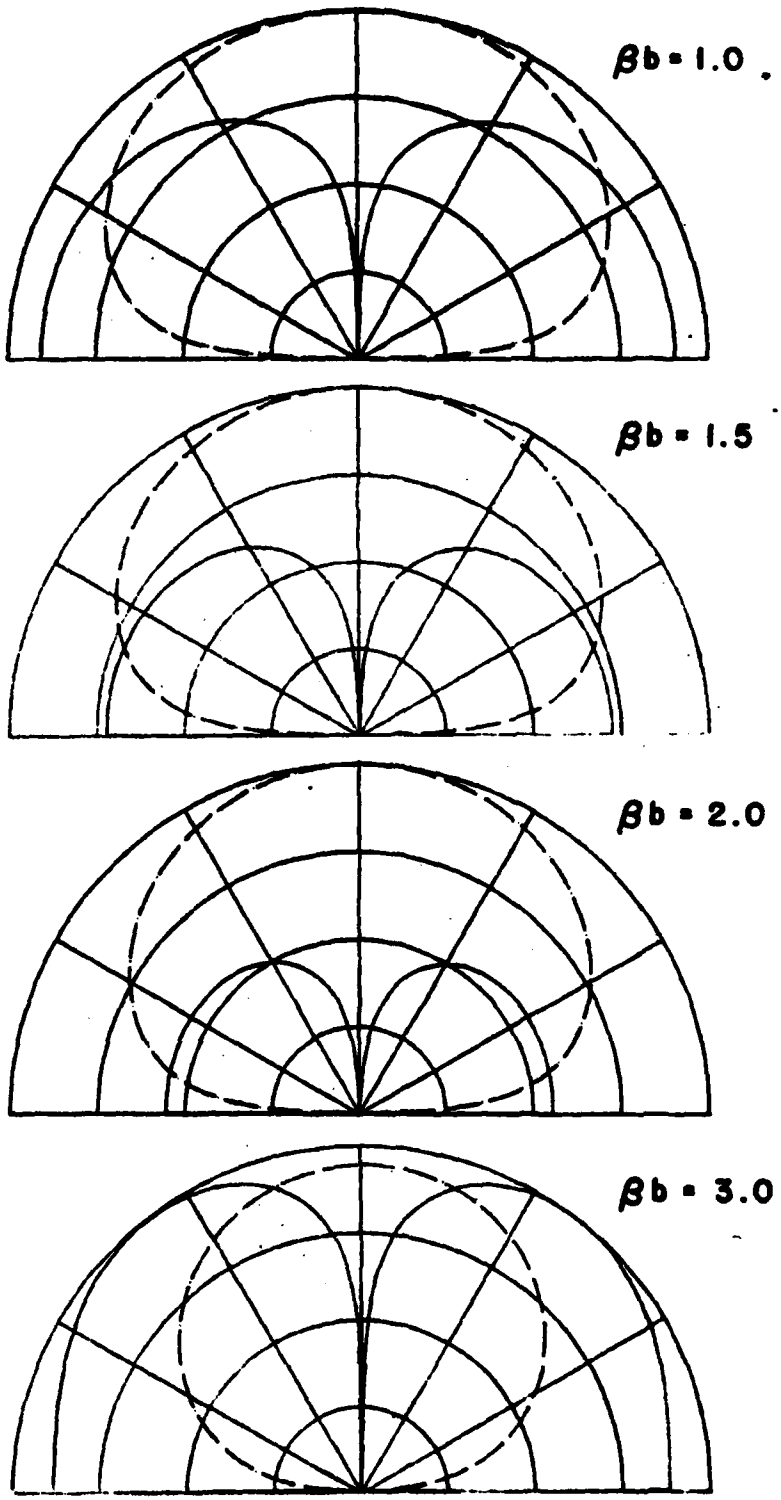

Figure 5-3. Vertical pattern at ϕ=90^{0}.

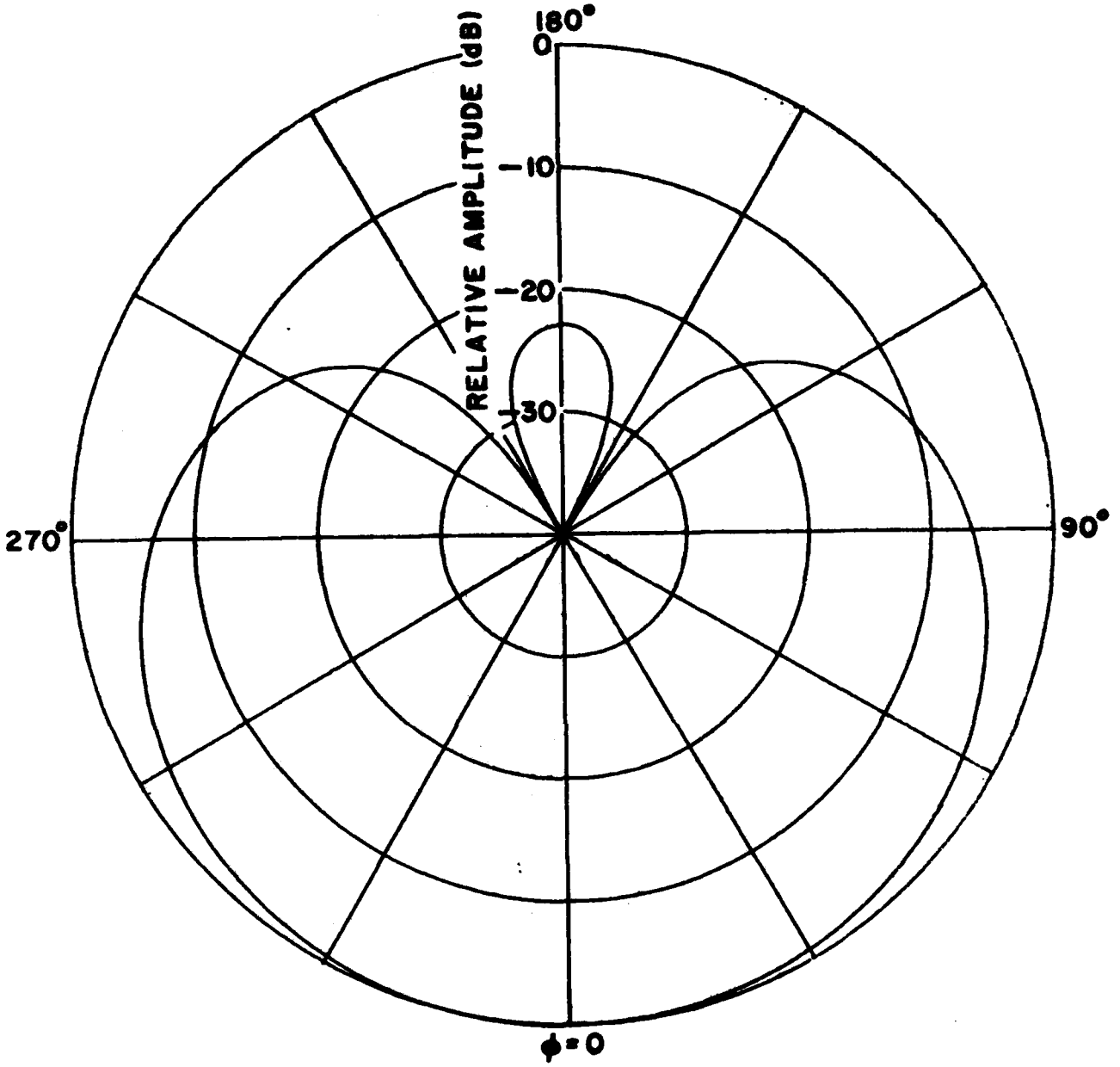

Figure 5-4. Horizontal pattern, null at $\pm 30^{0}$.

5.2 Cardioid condition

The cardioid condition is calculated using Equation (5-5). It is shown in Figure 5-5. In this diagram, $\Omega = 2\ell n\, 2\pi b/a$. As βb increases, locus of the cardioid condition changes considerably. This is another reason that a large loop is not favorable for this antenna.

5.3 Pattern change

The change in the horizontal pattern will now be observed as the feeding condition is shifted from the cardioid condition. Assume that amplitude becomes A times as much as before, and the the phase differs by δ radian. That is, the feeding voltage ratio is

$$V_b/V_a = V_b/V_a\Big|_{f_o} A\, e^{j\delta} \; ; \tag{5-11}$$

Substituting Equation (5-11), Equation (5-7) yields;

$$E_\phi(\pi/2,\phi) \sim 1 + j\,\frac{2\alpha_o}{\alpha_1}\,\frac{J_1'(\beta b)}{J_o'(\beta b)}\,\frac{1 - \dfrac{V_b}{V_a} A\, e^{j\delta}}{1 + \dfrac{V_b}{V_a} A\, e^{j\delta}}\cos \quad . \tag{5-12}$$

Figure 5-6a to Figure 5-6c show the case where δ is changed from -20^o to $+20^o$ by 10^o intervals with an A of 1.122(1dB), 1.0(0dB) and 0.891(-1dB).

Thus, we may conclude that this type of antenna is somewhat frequency sensitive.

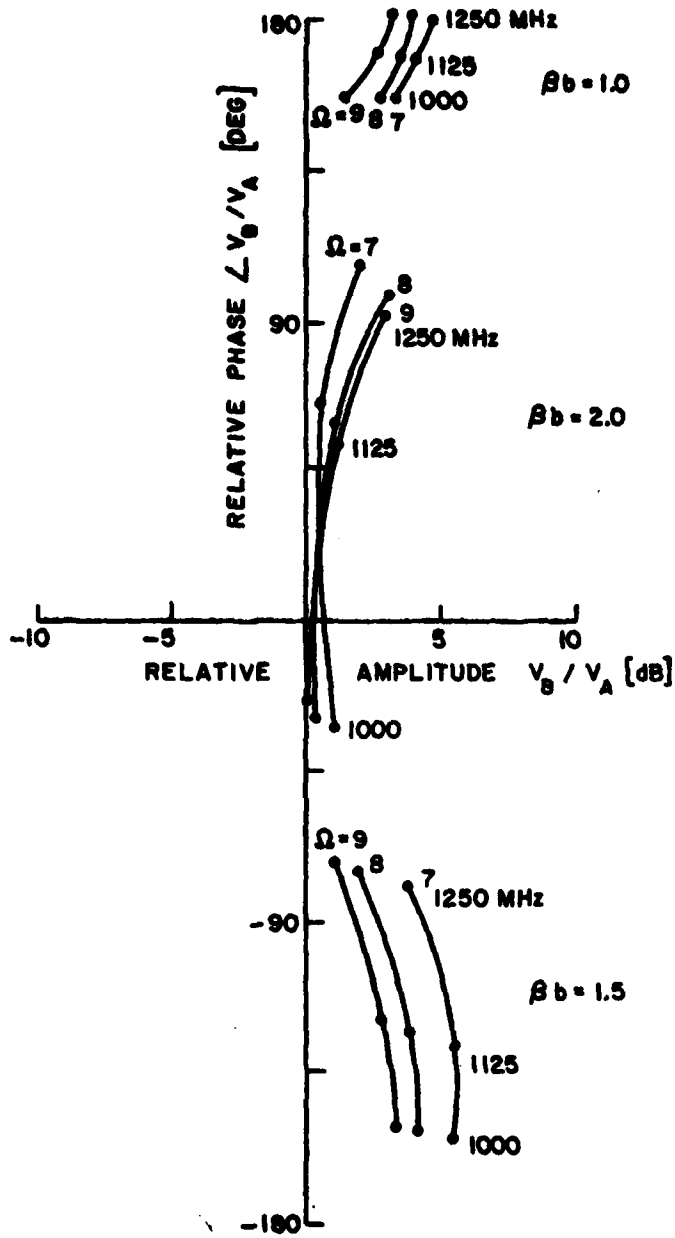

Figure 5-5. Cardioid condition.

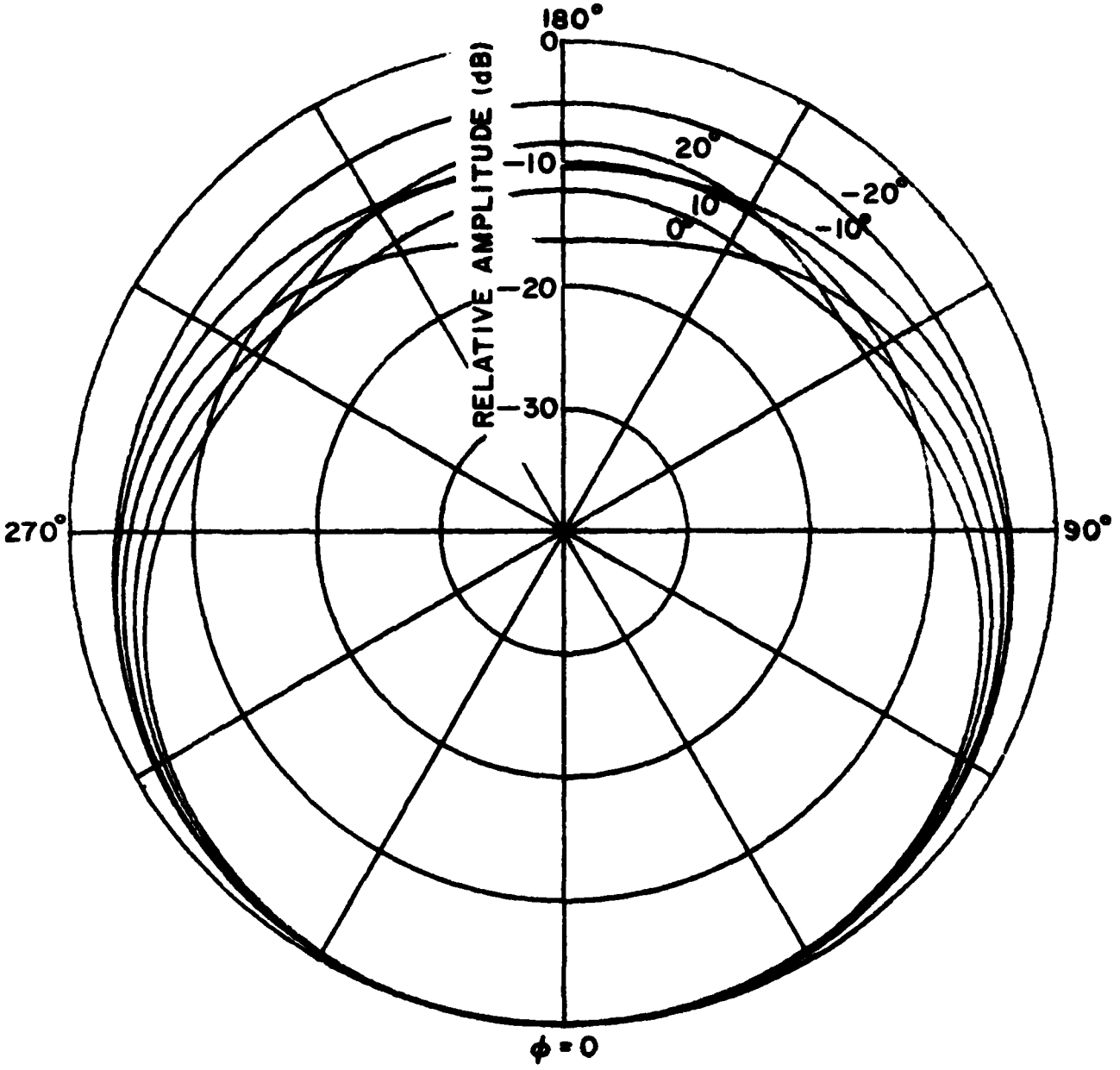

Figure 5-6(a) Pattern change.
Amplitude change: +1 dB.

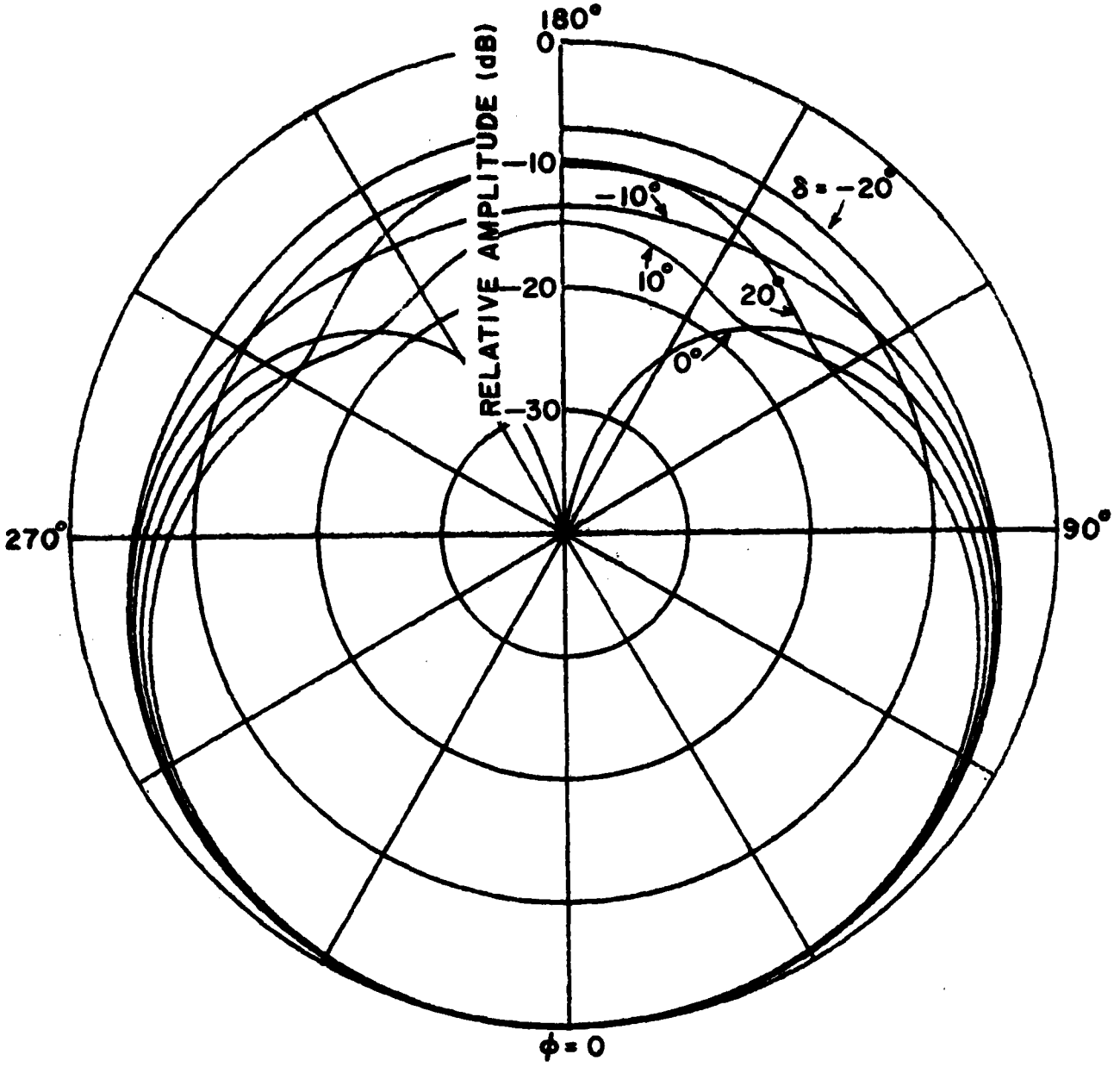

Figure 5-6(b). Pattern change.
Amplitude change: 0.

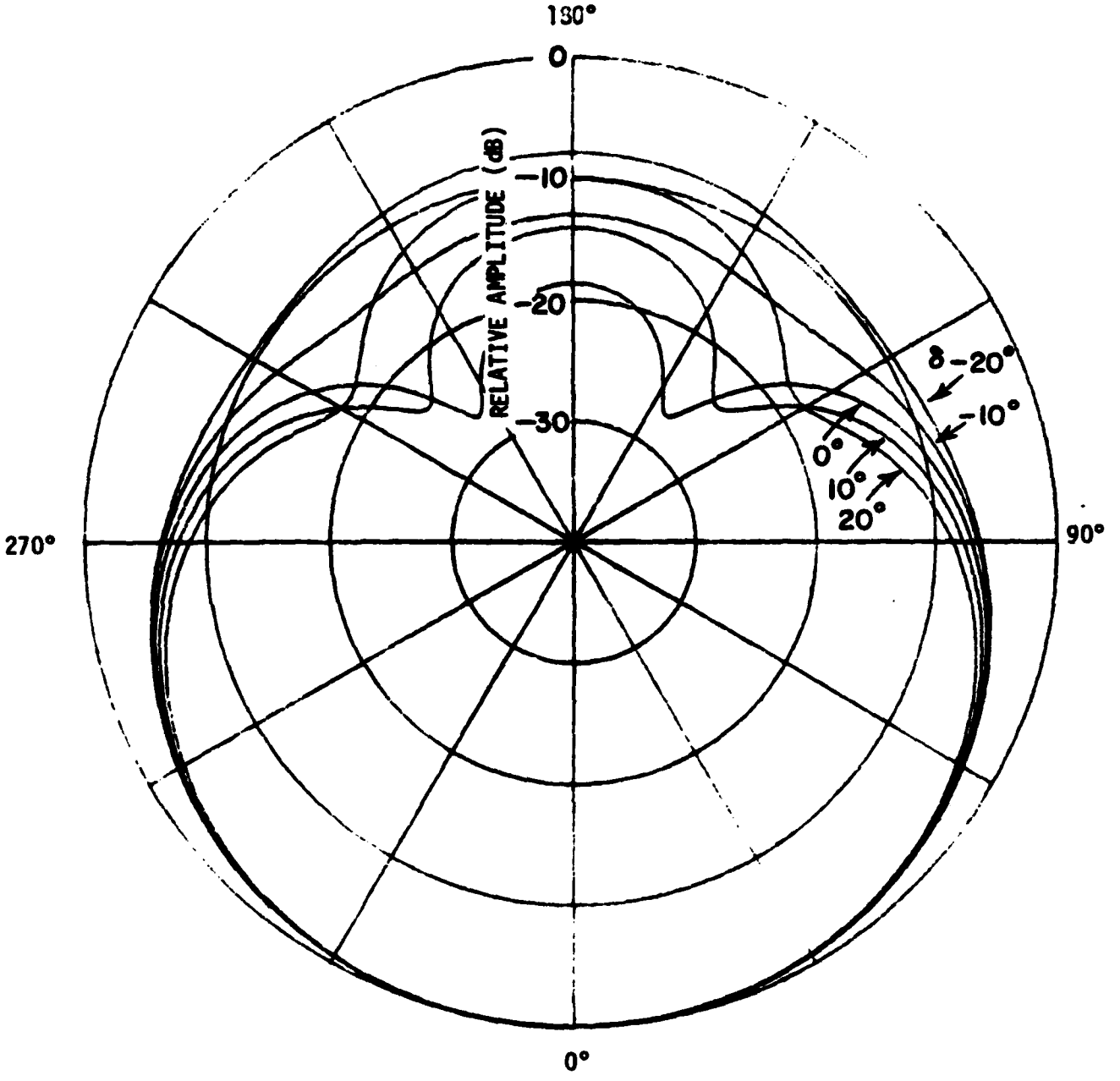

Figure 5-6(c). Pattern change.
Amplitude change: -1 dB.

6. TWO LOOPS FED AT TWO POINTS

6.1 Antenna pattern

This antenna consists of two concentric loops placed in the same plane (see Figure 6-1). A large outer loop operates the n=1 mode only, while a small inner loop operates the n=0 mode only. When the loop is driven by two generators as shown in Figure 2-5, the electric field in the horizontal plane is expressed by Equation (2-69) as

$$E_\phi(\pi/2,\phi) = \frac{Q\omega b}{\alpha_0} J_0'(\beta b)(V_a+V_b) + j\frac{2Q\omega b}{\alpha_1} J_1'(\beta b)(V_a-V_b)\cos\phi \qquad (6\text{-}1)$$

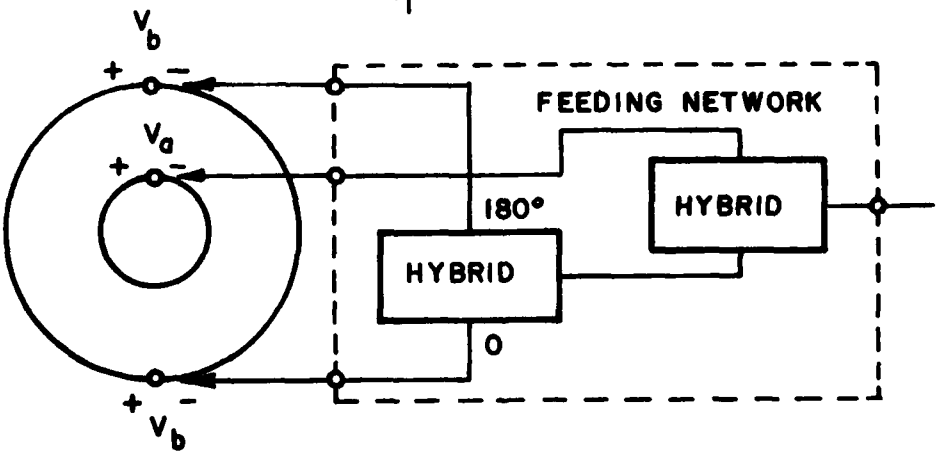

Figure 6-1. Two-loop antenna for cardioid pattern.

If $V_a=-V_b$, that is, equal in amplitude and 180^0 out of phase, the n=0 mode is eliminated and only the n=1 mode remains. If $V_a=V_b$, that is, equal in amplitude and phase, only the n=0 mode remains. Thus, n=1 in the outer loop and n=0 in the inner loop is possible. However, if the diameter of the loop is small, the n=0 mode is dominant. It

is not necessary for the inner loop to be driven by two in-phase generators. Figure 6-1 shows a possible configuration of this type of antenna. The electromagnetic field is the sum of the radiation by the inner and outer loops. The electric field in the horizontal plane is expressed as

$$E_\theta(\pi/2,\phi)=0 \tag{6-2}$$

$$E_\phi(\pi/2,\phi) = \frac{Q\omega b_{in}}{\alpha_0(in)} J_0'(\beta b_{in})V_a + j \frac{4Q\omega b_{out}}{\alpha_1(out)} J_1'(\beta b_{out}) V_b \cos\phi \tag{6-3}$$

where b_{in} = radius of inner loop
b_{out} = radius of outer loop
$\alpha_0(in)$ = 0th order coefficient of inner loop
$\alpha_1(out)$ = 1st order coefficient of outer loop.

The cardioid condition with null at $\phi=180^0$ is

$$E_\phi(\pi/2,\pi) = Q\omega \left[\frac{b_{in} J_0'(\beta b_{in})}{\alpha_0(in)} V_a - j \frac{4b_{out}}{\alpha_1(out)} J_1'(\beta b_{out}) V_b \right] = 0 \tag{6-4}$$

After the dimensions of the loop were chosen, the feeding network must satisfy the following relationship:

$$\frac{V_b}{V_a} = - \frac{j\ \alpha_1(out)}{4\ \alpha_0(in)} \frac{b_{in}}{b_{out}} \frac{J_0'(\beta b_{in})}{J_1'(\beta b_{out})} \tag{6-5}$$

Under this condition

$$E_\phi(\pi/2,\phi) = \frac{Q\omega b_{in}}{\alpha_0(in)} J_0'(\beta b_{in}) V_a[1 + \cos\phi] \qquad (6\text{-}6)$$

The general expressions for E_θ, and E_ϕ are obtained by summing the 0 mode from the inner loop and the contribution from the 1st mode on the outer loop and substituting (6-5) into these equations:

$$E_\theta(\theta,\phi) = \frac{j\omega Q V_b \, 4J_1(\beta b_{out}\sin\theta)\cos\theta\sin\phi}{\alpha_1(out)\beta\sin\theta}$$

$$= -\frac{\omega Q b_{in} J_0(\beta b_{in}) V_a J_1(\beta b_{out}\sin\theta)\cos\theta\sin\phi}{\alpha_0(in) b_{out} J_1(\beta b_{out})\beta\sin\theta} \qquad (6\text{-}7)$$

$$E_\phi(\theta,\phi) = \frac{\omega Q V_a b_{in} J_0'(\beta b_{in}\sin\theta)}{\alpha_0(in)} + \frac{j4\omega Q V_b b_{out} J_1(\beta b_{out}\sin\theta)\cos\phi}{\alpha_1(out)}$$

$$= -\frac{\omega Q b_{in} J_0'(\beta b_{in}\sin\theta)}{\alpha_0(in)} V_a \left[1 + \frac{J_1'(\beta b_{out}\sin\theta)}{J_0'(\beta b_{in}\sin\theta)} \frac{J_0'(\beta b_{in})}{J_1'(\beta b_{out})} \cos\phi\right] \qquad (6\text{-}8)$$

In particular for the horizontal plane, we obtain

$$E_\theta(\pi/2,\phi) = 0 \qquad (6\text{-}9)$$

$$E_\phi(\pi/2,\phi) = \frac{\omega Q b_{in} J_0'(\beta b_{in}) V_a}{\alpha_0(in)} \left[1+\cos\phi\right] \qquad (6\text{-}10)$$

The shape of this pattern shown in Figure 3-1 is of course the cardioid and is unchanged if the dimension of the loop is changed.

In the vertical plane $\phi=0$, we obtain

$$E_\theta(\theta,0) = 0 \tag{6-11}$$

$$E_\phi(\theta,0) = \frac{\omega Q b_{in} V_a}{\alpha_o(in)} \left[J_o'(\beta b_{in}\sin\theta) + J_1'(\beta b_{out}\sin\theta) \frac{J_o'(\beta b_{in})}{J_1'(\beta b_{out})} \right] \tag{6-12}$$

This radiation pattern is shown in Figure 6-2 for various βb. Note, that null appears in the elevation direction when $\beta b=2.0$. This shows that a large diameter is not desirable for this antenna. In the plane $\phi=90^o$ we obtain

$$E_\theta(\theta,\pi/2) = \frac{\omega Q b_{in}}{\alpha_o(in)} \frac{J_o(\beta b_{in})}{J_1(\beta b_{out})} \frac{V_a J_1(\beta_{bout}\sin\theta)\cos\theta}{\beta_{bout}\sin\theta} \tag{6-13}$$

$$E_\phi(\theta,\pi/2) = \frac{\omega Q V_a\, b_{in}\, J_o'(\beta b_{in}\sin\theta)}{\alpha_o(in)} \tag{6-14}$$

This radiation pattern is shown in Figure 6-3 for various βb.

6.2 Change of The Cardioid Condition

The cardioid condition is given by Equation (6-4). This value is a function of frequency and the size of the loop. How the cardioid condition changes with frequency is now investigated. The results are shown in Figure 6-4. The radius b of outer loop is selected to be $\beta b=1.0$, 1.5 and 2.0. The radius a of the wire is selected to be $\Omega=7$, 8 and 9.

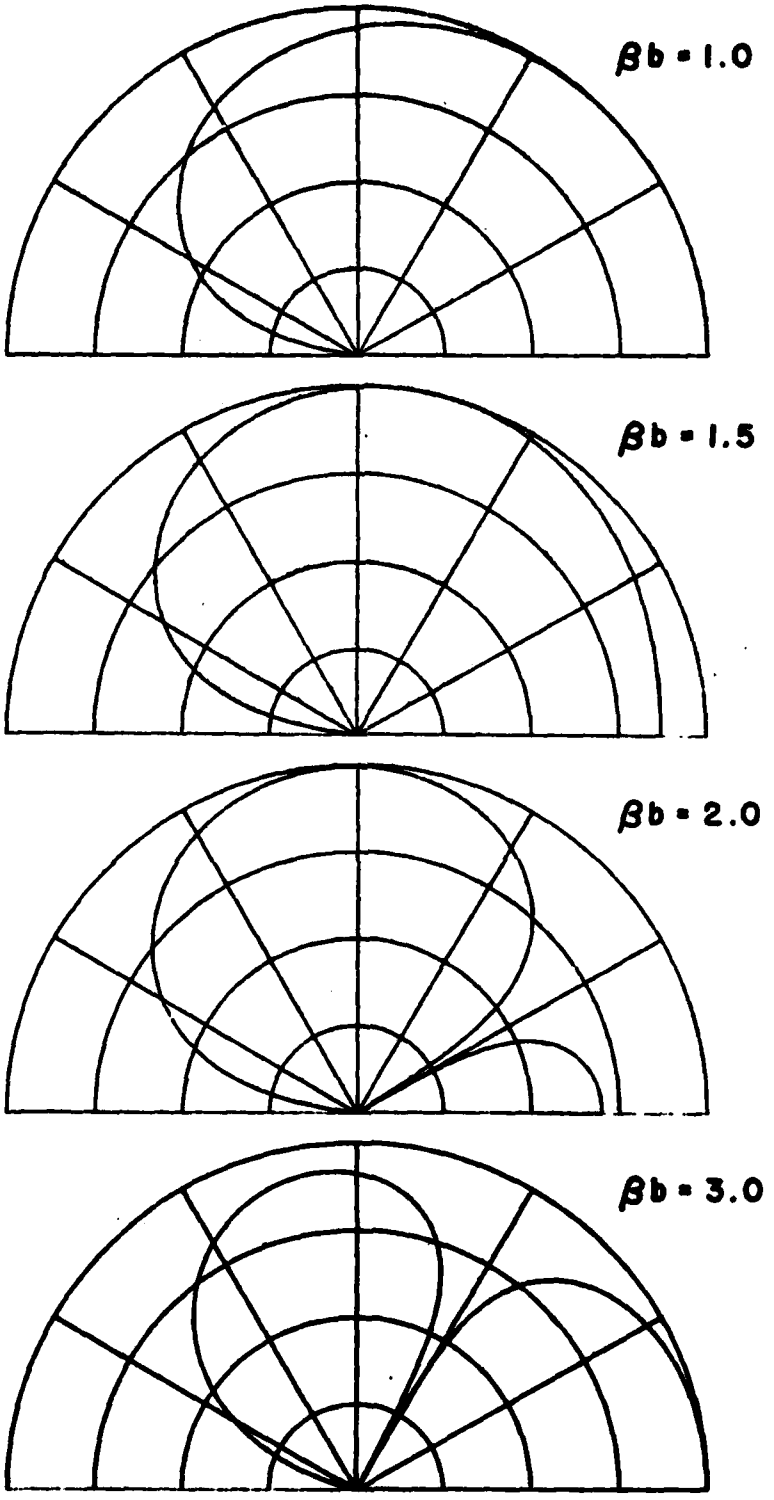

Figure 6-2. Vertical pattern at $\phi = 0^{\circ}$.

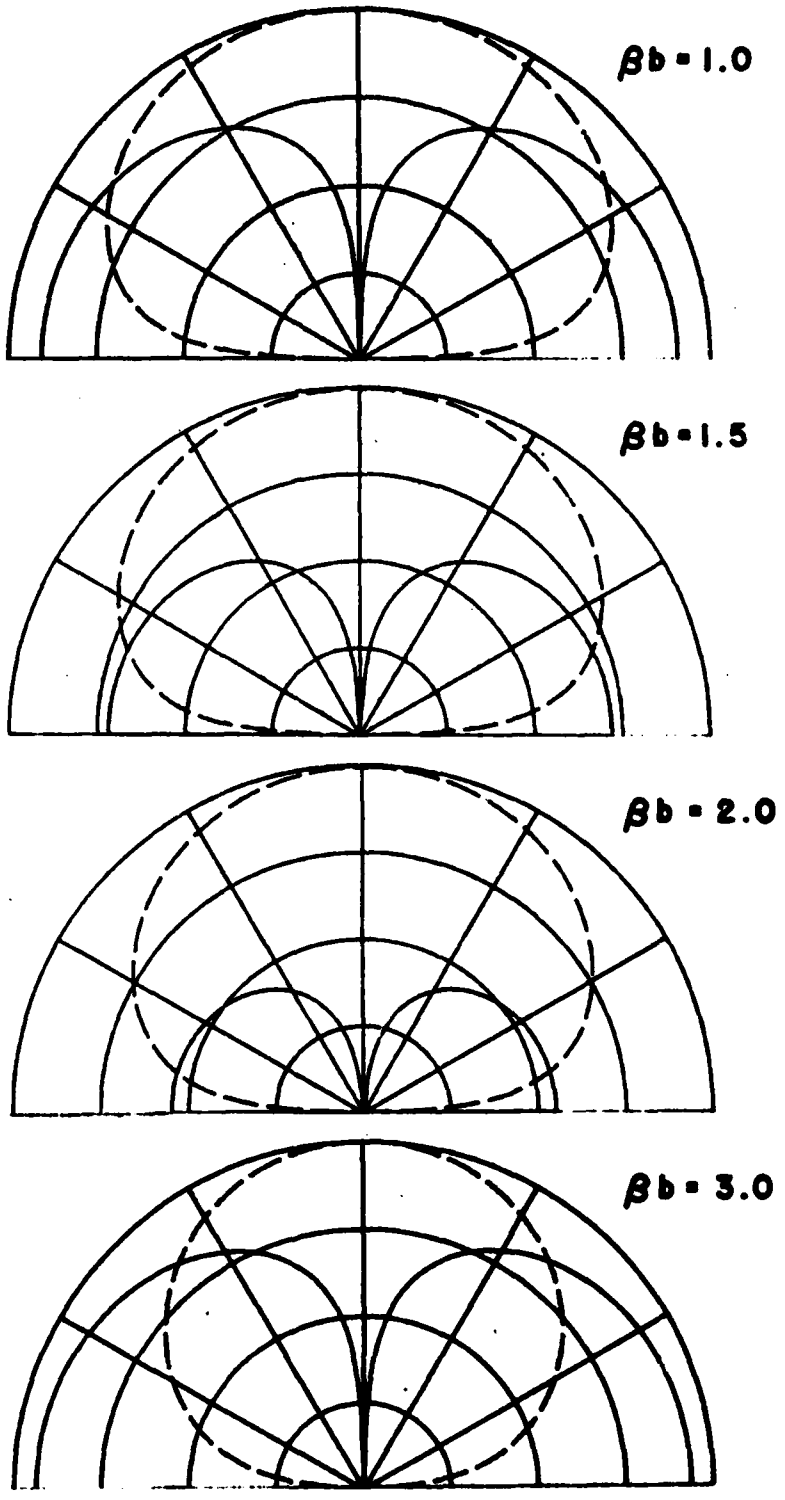

Figure 6-3. Vertical pattern at $\phi=90^{0}$.

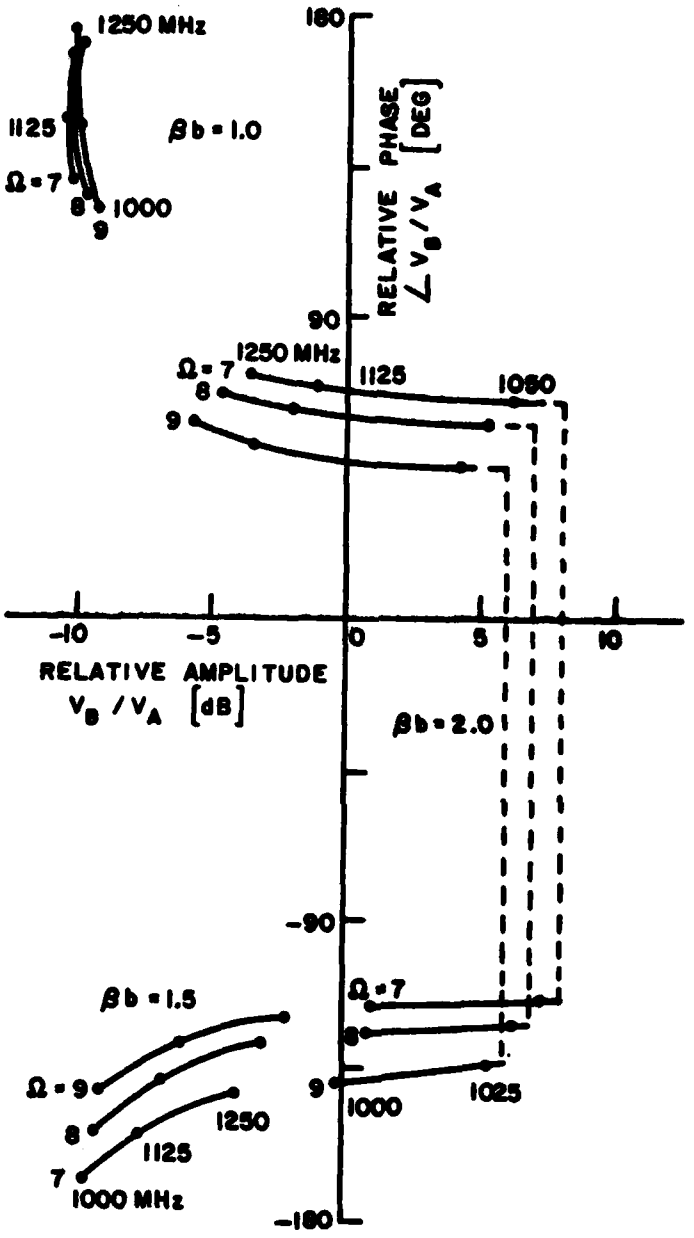

Figure 6-4. Cardiod condition.

The horizontal axis is the voltage ratio $|V_b/V_a|$.
The vertical axis is the phase difference $\angle V_b/V_a$.

For $\beta b=1.0$, the voltage is a constant while the phase changes with frequency. Therefore it is desirable that the feeding network compensate for the phase change, if the cardioid pattern is expected over the entire frequency range. A possible feeding network is realized by using transmission lines. However, in the case of $\beta b=2.0$ the cardioid condition moves along the constant phase line, and the phase suddenly gets 180^0 out of phase. This is one reason that a large diameter loop cannot be used as this type of antenna. The other reason is the null in the elevation as stated earlier. In the $\beta b=1.5$ case the situation is for the middle of the two cases. Both voltage and phase change according to frequency.

6.3 Change of Pattern

In this section we will consider the change in pattern for various parameter changes. The electric field $E_\phi(\pi/2,\phi)$ in the horizontal plane is given by Equation (6-3). It is rewritten as,

$$E_\phi(\pi/2,\phi) \sim 1 + c(f)\,\frac{V_b}{V_a}\cos\phi \qquad (6\text{-}15)$$

where

$$c(f) = j4\,\frac{\alpha_0(in)}{\alpha_1(out)}\;\frac{b_{out}}{b_{in}}\;\frac{J_1'(\beta b_{out})}{J_0'(\beta b_{in})} \qquad (6\text{-}16)$$

The cardioid condition is

$$\frac{V_b}{V_a} = -\frac{1}{c(f)} \quad . \qquad (6\text{-}17)$$

The feeding network must be designed to satisfy Equation (6-17) at the center frequency f_o. However, at a frequency different from the center frequency, α_o, α_1, β and $c(f)$ are different from those of the center frequency. $c(f)$ is assumed to be different from $c(f_o)$ by A times in amplitude and δ radians in phase, i.e.,

$$c(f) = c(f_o) \quad A\, e^{j\delta} \tag{6-18}$$

The feeding network also has frequency characteristics. But the feeding network here is assumed to keep V_b/V_a constant. Under such circumstances

$$\begin{aligned} E_\phi(\pi/2, \phi) &\sim 1 + c(f)\, V_b/V_a \cos\phi \\ &\sim 1 + c(f_o)\, A\, e^{j\delta}\, V_b/V_a \cos\phi \\ &\sim 1 + A\, e^{j\delta} \cos\phi \end{aligned} \tag{6-19}$$

where relationship (6-17) is used.

Equation (6-19) is also true in the following case. At the center frequency f_o the feeding network has some error and $V_b/V_a = -\frac{1}{c(f_o)}\, A\, e^{j\delta}$. The error is A times in amplitude and δ radian in phase. The result of this calculation is shown in Figure 6-5. For example in the case f=1125 MHz, βb=1.0 and Ω=8, V_b/V_a at cardioid condition is -10.5 dB, 148^o from Figure 6-4. When frequency is shifted to 1250 MHz, V_b/V_a becomes -10.3 dB, 173^o. The difference of V_b/V_a is 0.2 dB, 25^o. If the feeding network is frequency independent, the anticipated pattern will be a curve between $\delta=20^o$ and $\delta=30^o$ in Figure 6-5(b).

If the feeding network is frequency dependent and the phase is shifted by -15^o, the difference of V_b/V_a is 0.2 dB, -10^o. The pattern in that case is a curve of -10^o in Figure 6-5(b).

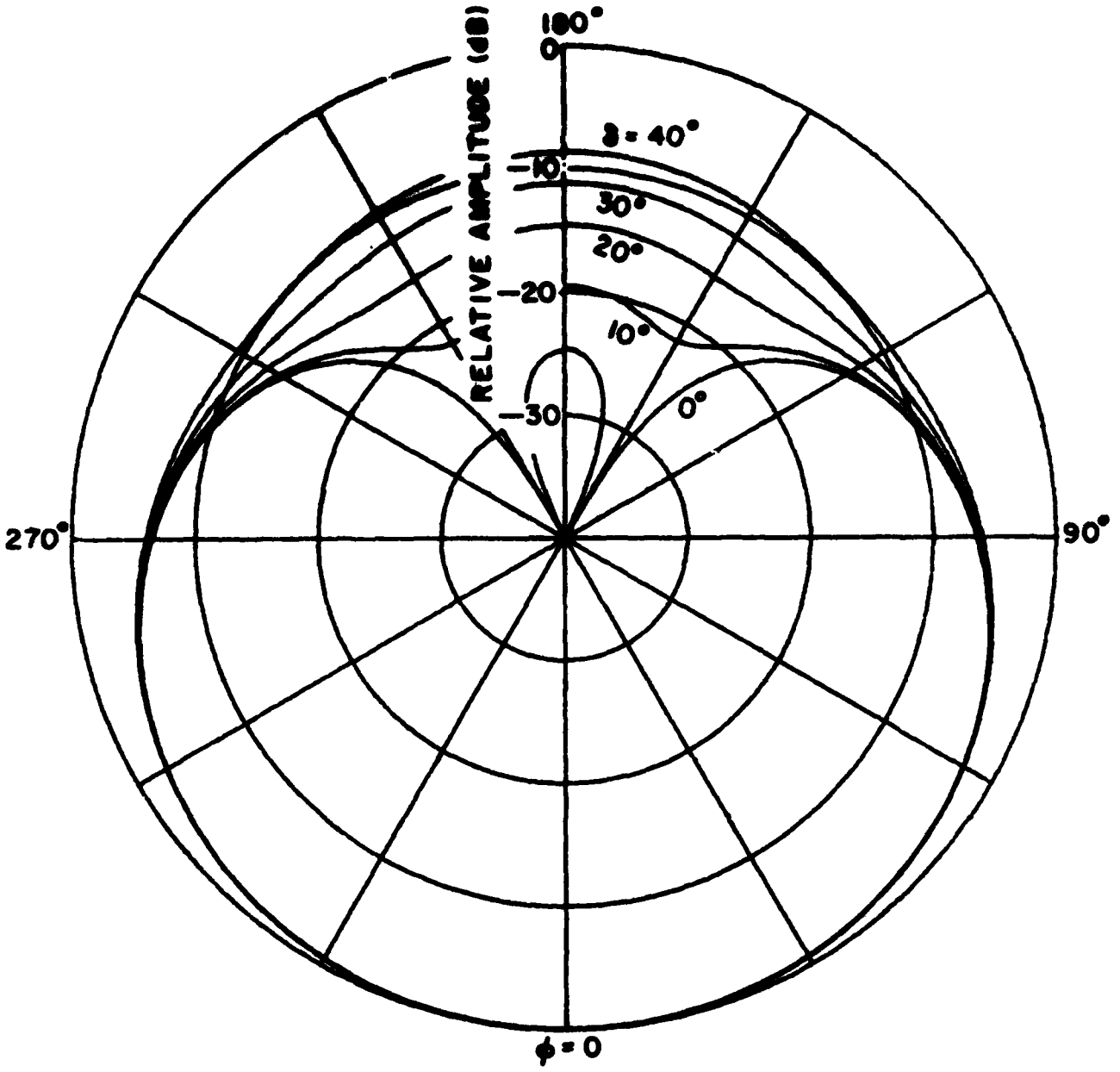

Figure 6-5(a) Pattern change.
Amplitude change: +1 dB.

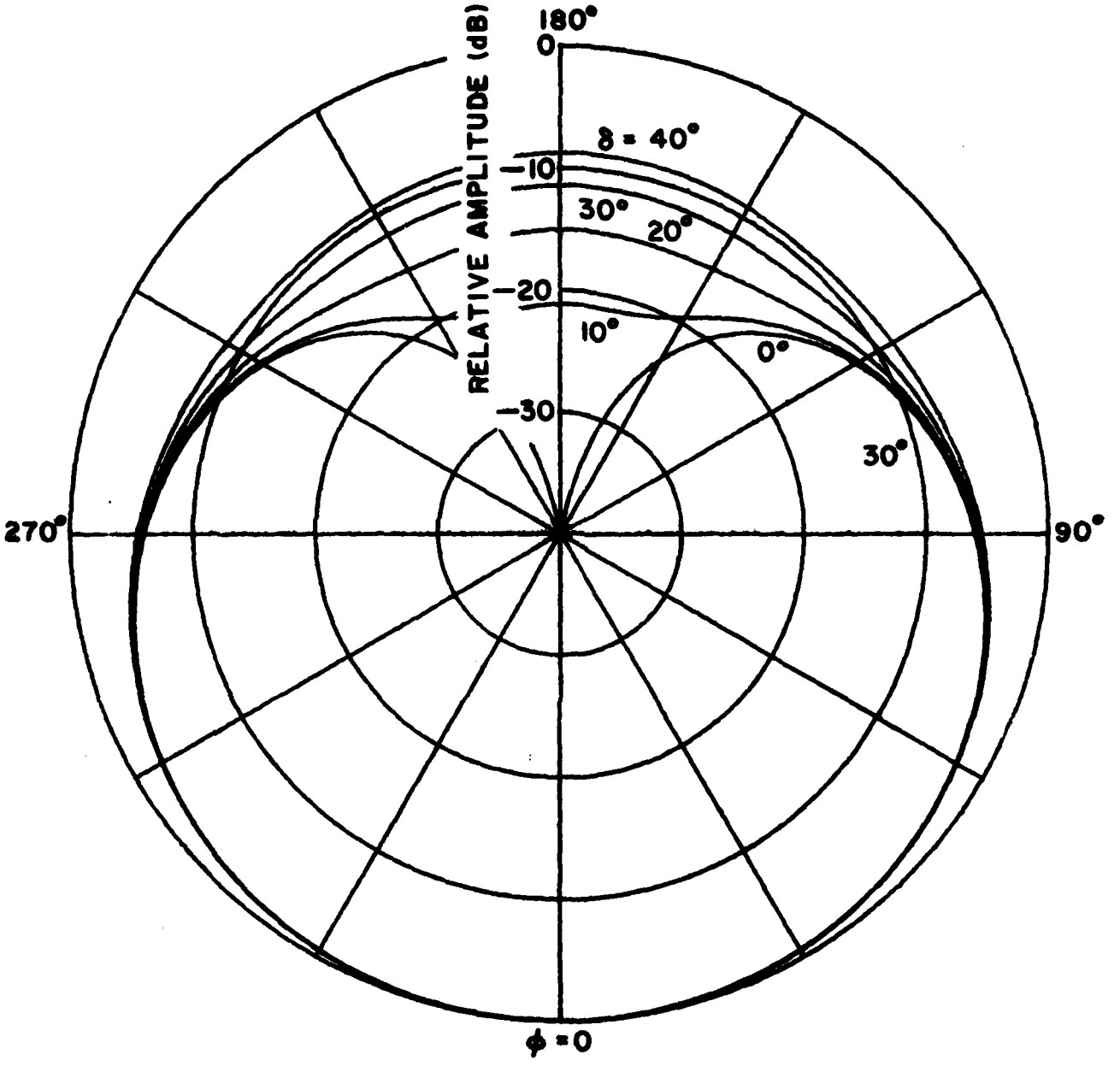

Figure 6-5(b). Pattern change.
Amplitude change: 0.

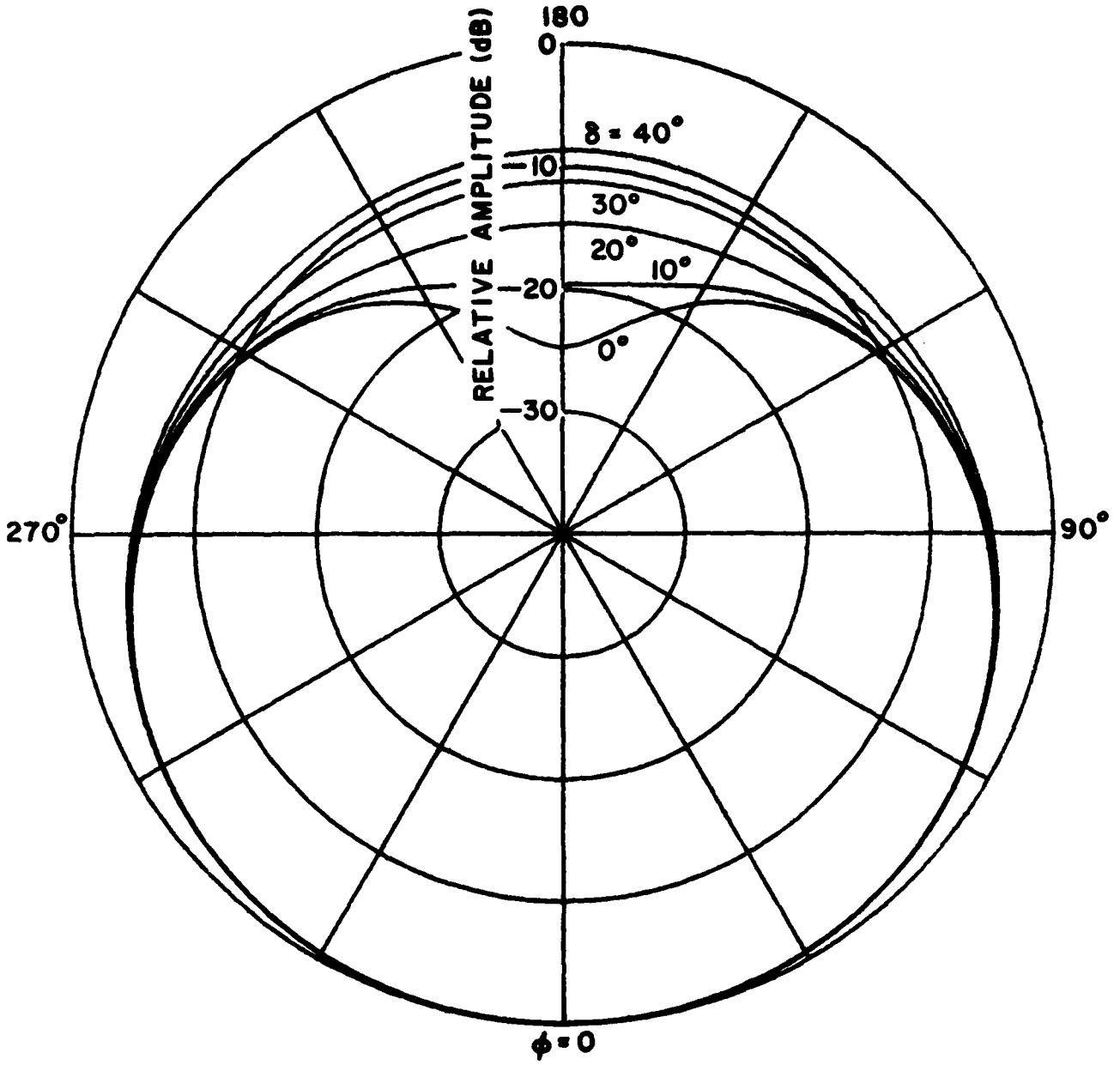

Figure 6-5(c) Pattern change.
Amplitude change: -1 dB.

6.4 Feeding Network Consideration

We shall now determine how much deviation from the cardioid condition is permissible if the front-to-back ratio (FBR) is given. The electric field $E_\phi(\pi/2,\phi)$ in the $\theta=\pi/2$ plan is the same as (6-15)

$$E_\phi(\pi/2,\phi) \sim 1 + c(f)\,\frac{V_b}{V_a}\cos\phi \tag{6-20}$$

FBR is defined as

$$\begin{aligned} FBR &= 20\log_{10}\left|\frac{E_\phi(\pi/2,0)}{E_\phi(\pi/2,\pi)}\right| \\ &= 20\log_{10}\left|\frac{1 + c(f)\,\frac{V_b}{V_a}}{1 - c(f)\,\frac{V_b}{V_a}}\right| \end{aligned} \tag{6-21}$$

$$\left|\frac{1 + c(f)\,\frac{V_b}{V_a}}{1 - c(f)\,\frac{V_b}{V_a}}\right| = 10^{FBR/20} = K \tag{6-22}$$

From the cardioid condition,

$$1 - c(f_o)\,\frac{V_b}{V_a}\bigg|_{f_o} = 0 \tag{6-23}$$

We now assume the feeding condition is changed to

$$\frac{V_b}{V_a} = \frac{V_b}{V_a}\bigg|_{f_o} A e^{j\delta} = \frac{1}{C(f_o)}\,A e^{j\delta}$$

in the same manner as before. Thus Equation (6-22) is reduced to

$$\left| \frac{1 + A\, e^{j\delta}}{1 - A\, e^{j\delta}} \right| = K. \tag{6-24}$$

If the FBR is given, permissible range of A without phase shift is

$$\left| \frac{1 + A}{1 - A} \right| > K$$

that is

$$\frac{K + 1}{K - 1} > A > \frac{K - 1}{K + 1} \tag{6-25}$$

Permissible range of δ without amplitude change is

$$\left| \frac{1 + e^{j\delta}}{1 - e^{j\delta}} \right| > K$$

$$\cos^{-1} \frac{K^2 - 1}{K^2 + 1} > \delta > - \cos^{-1} \frac{K^2 - 1}{K^2 + 1} \tag{6-26}$$

When both A and δ are changed, the permissible range is

$$\left| \frac{1 + A\, e^{j\delta}}{1 - A\, e^{j\delta}} \right| > K \tag{6-27}$$

$$\frac{A}{2} + \frac{1}{A} < \frac{K^2 + 1}{K^2 - 1} \cos\delta \tag{6-28}$$

This curve is shown in Figure 6-6 where we note the permissible range of amplitude and phase when the FBR is given. Combining Figure 6-4 and Figure 6-5, we obtain the range of V_b/V_a. We now draw the FBR circle for cardioid condition at each frequency as shown in Figure 6-7 for $\beta b=1.0$, $\Omega=8$. A frequency range from 1.0 GHz to 1.25 GHz is assumed in Figure 6-7. If V_b/V_a is chosen in the shadow regions, the requirement of 15 dB FBR at the frequency range between 1.0 to 1.25 GHz and between 1.125 and 1.25 GHz will be satisfied. However both regions do not overlap so there is no way to change the ratio V_b/V_a such that it will satisfy the entire frequency range from 1.0 to 1.25 GHz. To do this, the feeding network should be designed to compensate for cardioid condition changes.

7. TWO LOOPS FED AT FOUR POINTS

7.1 Antenna patterns

There is an alternate method to obtain the quasi-cardioid pattern in a dual loop. The outer loop is fed at four points with progressive phase as shown in Figure 7-1. The resultant electromagnetic field is the sum of each contribution as derived in Section 2.3. E_ϕ is obtained by use of Equation (2-56) as follows.

$$E_\phi = \omega Q V_o\, b\left[\frac{J_o'(\beta b\sin\theta)}{\alpha_o} + j\,\frac{2J_1'(\beta b\sin\theta)}{\alpha_1}\cos\phi\right]$$

$$+ \omega Q(-jV_o)b\left[\frac{J_o'(\beta b\sin\theta)}{\alpha_o} + j\,\frac{2J_1(\beta b\sin\theta)}{\alpha_1}\cos(\phi+\pi/2)\right]$$

$$+ \omega Q(-V_o)b\left[\frac{J_o'(\beta b\sin\theta)}{\alpha_o} + j\,\frac{2J_1'(\beta b\sin\theta)}{\alpha_1}\cos(\phi+\pi)\right]$$

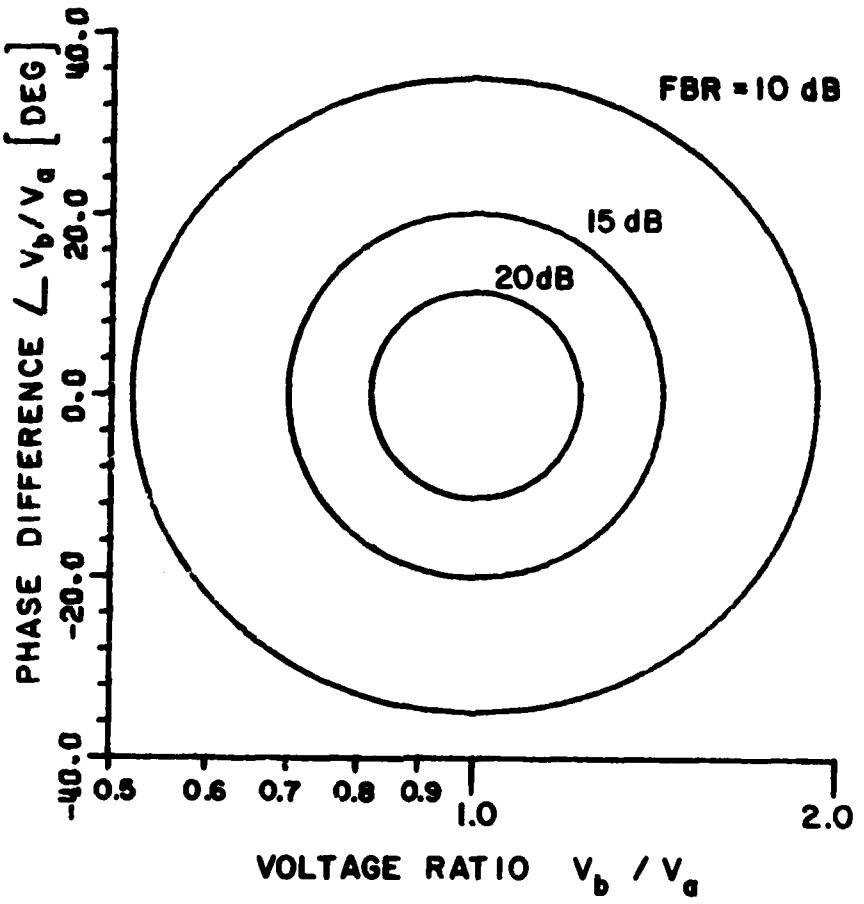

Figure 6-6. Diagram showing the acceptance range for feeding variation.

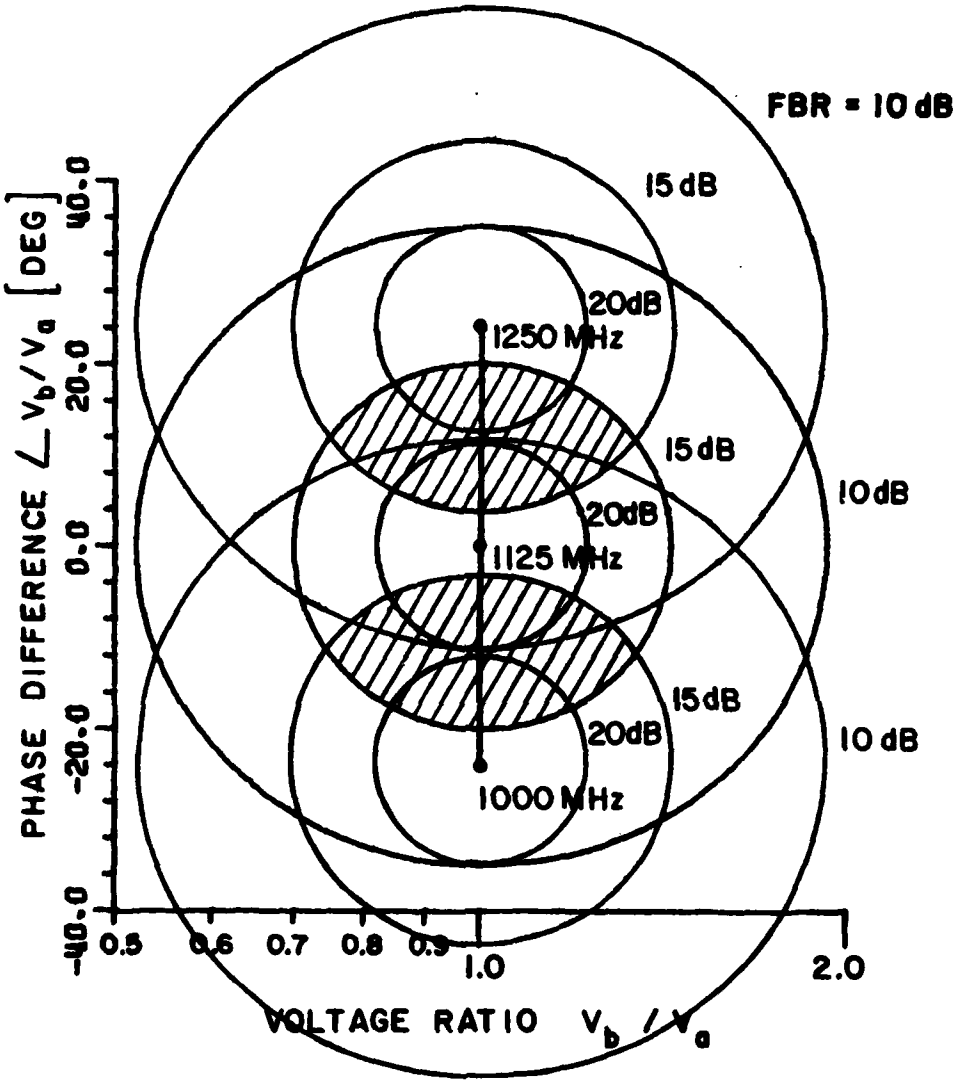

Figure 6-7. Determination for feeding condition.

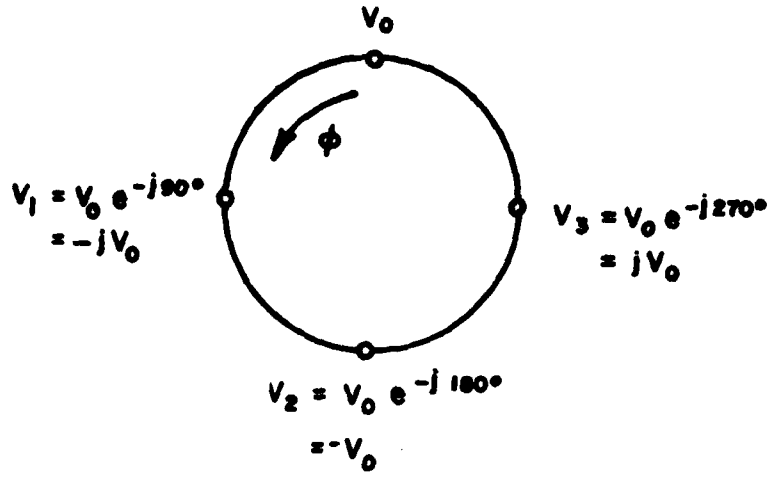

Figure 7-1. Feeding condition to obtain the element distribution $e^{j\phi}$.

$$+ \omega Q(jV_0)b\left[\frac{J_0'(\beta b\sin\theta)}{\alpha_0} + j\,\frac{2J_1'(\beta b\sin\theta)}{\alpha_1}\cos(\phi+3\pi/2)\right]$$

$$E_\phi = j\,\frac{4\omega QV_0 bJ_1'(\beta b\sin\theta)}{\alpha_1}(\cos\phi+j\sin\phi)$$

$$= j\,\frac{4\omega QV_0 bJ_1'(\beta b\sin\theta)}{\alpha_1}\,e^{j\phi} \qquad (7\text{-}1)$$

If the small loop which radiates omnidirectionally is placed in the large loop as shown in Figure 7-2, the total electric field is

$$E_\phi(\theta,\phi) = \frac{\omega QV_a b_{in}\,J_0'(\beta b_{in}\sin\theta)}{\alpha_0(in)}$$

$$+ j\,\frac{4\omega QV_b\,b_{out}\,J_1'(\beta b_{out}\sin\theta)}{\alpha_1(out)}\,e^{j\phi} \qquad (7\text{-}2)$$

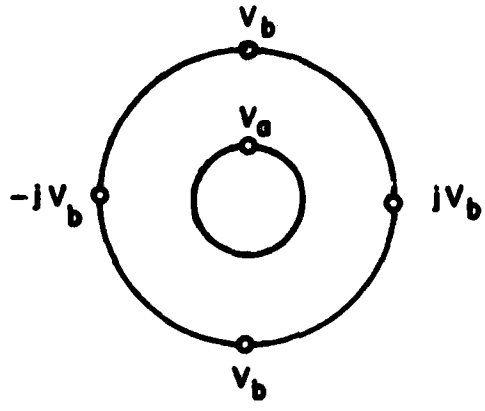

Figure 7-2. Two-loop antenna fed at four points.

The condition for a null in the $\phi=\pi$ direction in the horizontal plane is

$$E_\phi(\pi/2,\pi) = \omega Q\left[\frac{V_a b_{in} J_0'(\beta b_{in})}{\alpha_0(in)} - j\,\frac{4V_b b_{out} J_1'(\beta b_{out})}{\alpha_1(out)}\right] = 0 \quad (7\text{-}3)$$

or

$$\frac{V_b}{V_a} = j\,\frac{\alpha_1(out)}{4\alpha_0(in)}\,\frac{b_{in}}{b_{out}}\,\frac{J_0'(\beta b_{in})}{J_1'(\beta b_{out})} \quad (7\text{-}4)$$

Note that the cardioid condition (7-4) is exactly the same as that of two-point-drive in dual loop (6-6). Under this condition the horizontal pattern is

$$E_\phi(\pi/2,\phi) = \frac{\omega Q V_a J_o'(\beta b_{in})}{\alpha_o(in)}[1 + e^{\phi}] \quad . \tag{7-5}$$

This pattern is shown in Figure 7-3. There are two curves in this figure. An explanation is given in the next section. The same procedure leads to the following equation concerning E_θ:

$$E_\theta(\theta,\phi) = \frac{4\omega Q V_b J_1(\beta b_{out}\sin\theta)\cos\theta}{\alpha_1(out)\beta \sin\theta} e^{j\phi} \tag{7-5}$$

The general expressions for E_θ, E_ϕ at cardioid condition are

$$E_\phi(\theta,\phi) = -\frac{\omega Q V_a b_{in} J_o'(\beta b_{in}\sin\theta)}{\alpha_o(in)}\left[1 + j\,4\,\frac{b_{out}}{b_{in}}\,\frac{\alpha_o(in)}{\alpha_1(out)}\,\frac{J_1'(\beta b_{out}\sin\theta)}{J_o'(\beta b_{in}\sin\theta)}\,\frac{V_b}{V_a}\,e^{j\phi}\right] \tag{7-6}$$

or by use of Equation (7-4),

$$E_\phi(\theta,\phi) = \frac{\omega Q V_a b_{in} J_o'(\beta b_{in}\sin\theta)}{\alpha_o(in)}\left[1 + \frac{J_o'(\beta b_{in})}{J_1'(\beta b_{out})}\,\frac{J_1'(\beta b_{out}\sin\theta)}{J_o'(\beta b_{in}\sin\theta)}\,e^{j\phi}\right] \tag{7-7}$$

$$E_\theta(\theta,\phi) = \frac{\omega Q V_a b_{in} J_o'(\beta b_{in}\sin\theta)}{\alpha_o(in)} \times 4\,\frac{\alpha_o(in)}{\alpha_1(out)}\,\frac{\cos\theta}{b_{in}\sin\theta} \times \frac{J_1(\beta b_{out}\sin\theta)}{J_o'(\beta\, b_{in}\sin\theta)}\,\frac{V_b}{V_a}\,e^{j\phi} \tag{7-8}$$

or by Equation (7-4)

$$E_\theta(\theta,\phi) = \frac{\omega Q V_a b_{in} J_o'(\beta b_{in}\sin\theta)}{\alpha_o(in)}$$

$$\times \frac{\cos\theta}{\beta b_{out}\sin\theta} \frac{J_o'(\beta b_{in})}{J_1'(\beta b_{out})} \frac{J_1'(\beta b_{out}\sin\theta)}{J_o'(\beta b_{in}\sin\theta)} e^{j\phi} \quad (7\text{-}9)$$

The vertical patterns in the planes $\phi=0$ and $\phi=\pi/2$ are shown in Figures 7-4 and 7-5, respectively.

7.2 Change of pattern

Assume now that the feeding condition is changed from (7-4) to

$$\frac{V_b}{V_a} = \frac{V_b}{V_a}\Big|_{f_o} Ae^{j\delta}$$

$$= \frac{\alpha_1(out)}{4\alpha_o(in)} \frac{b_{in}}{b_{out}} \frac{J_o'(\beta b_{in})}{J_1'(\beta b_{out})} Ae^{j\delta} \quad . \quad (7\text{-}11)$$

The horizontal pattern then becomes

$$E_\phi(\pi/2,\phi) \sim 1 + Ae^{j\delta}e^{j\phi} \quad . \quad (7\text{-}12)$$

If the amplitude ratio remains constant, that is A=1, then

$$E_\phi(\pi/2,\phi) \sim 1 + e^{j(\phi+\delta)} \quad . \quad (7\text{-}13)$$

This is the same pattern as (7-5) except that a null occurs at $\phi=\pi-\delta$. Phase change affects only the position of null. In Figure 7-3, the

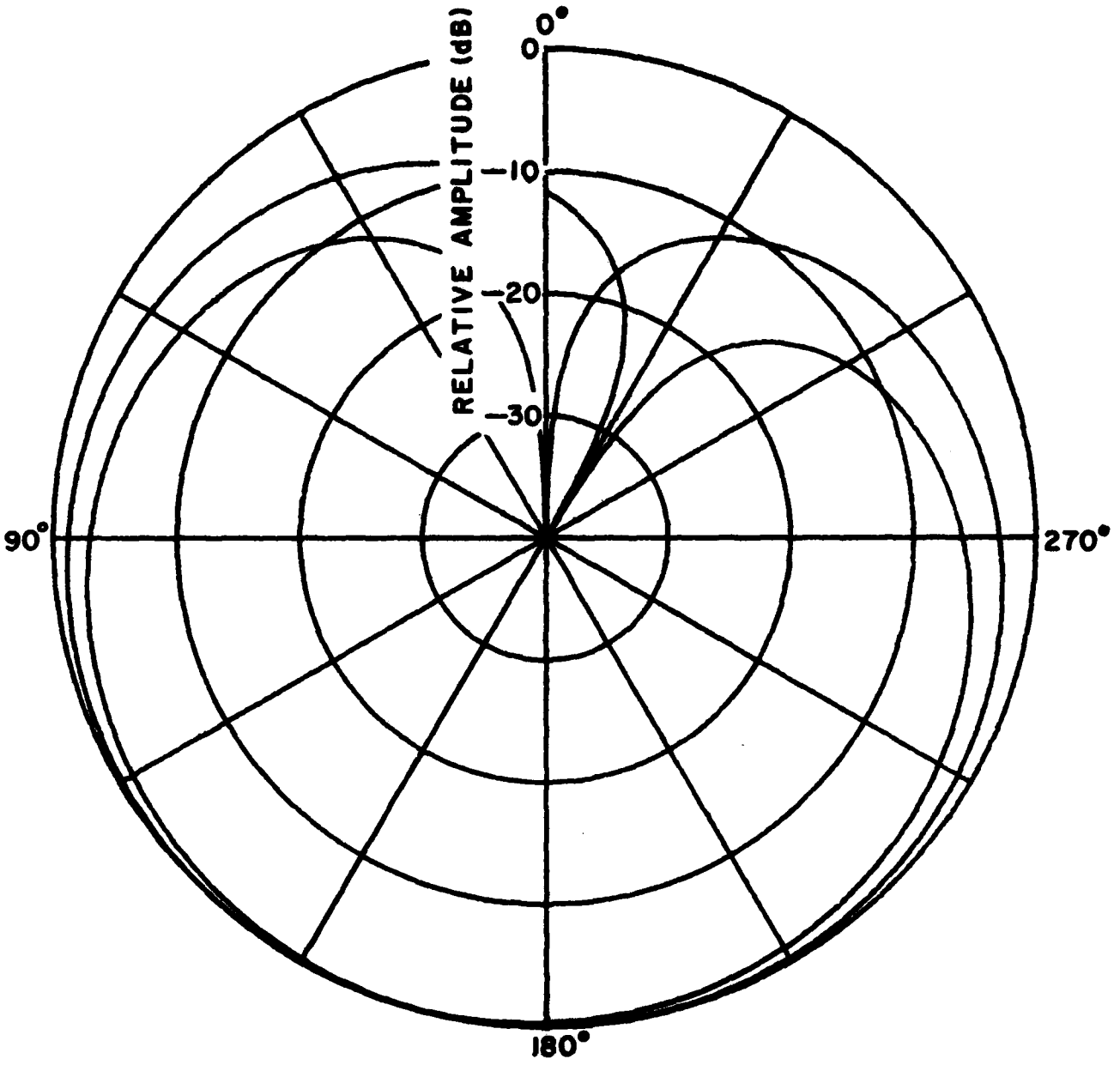

Figure 7-3. Horizontal pattern including pattern change due to phase change.

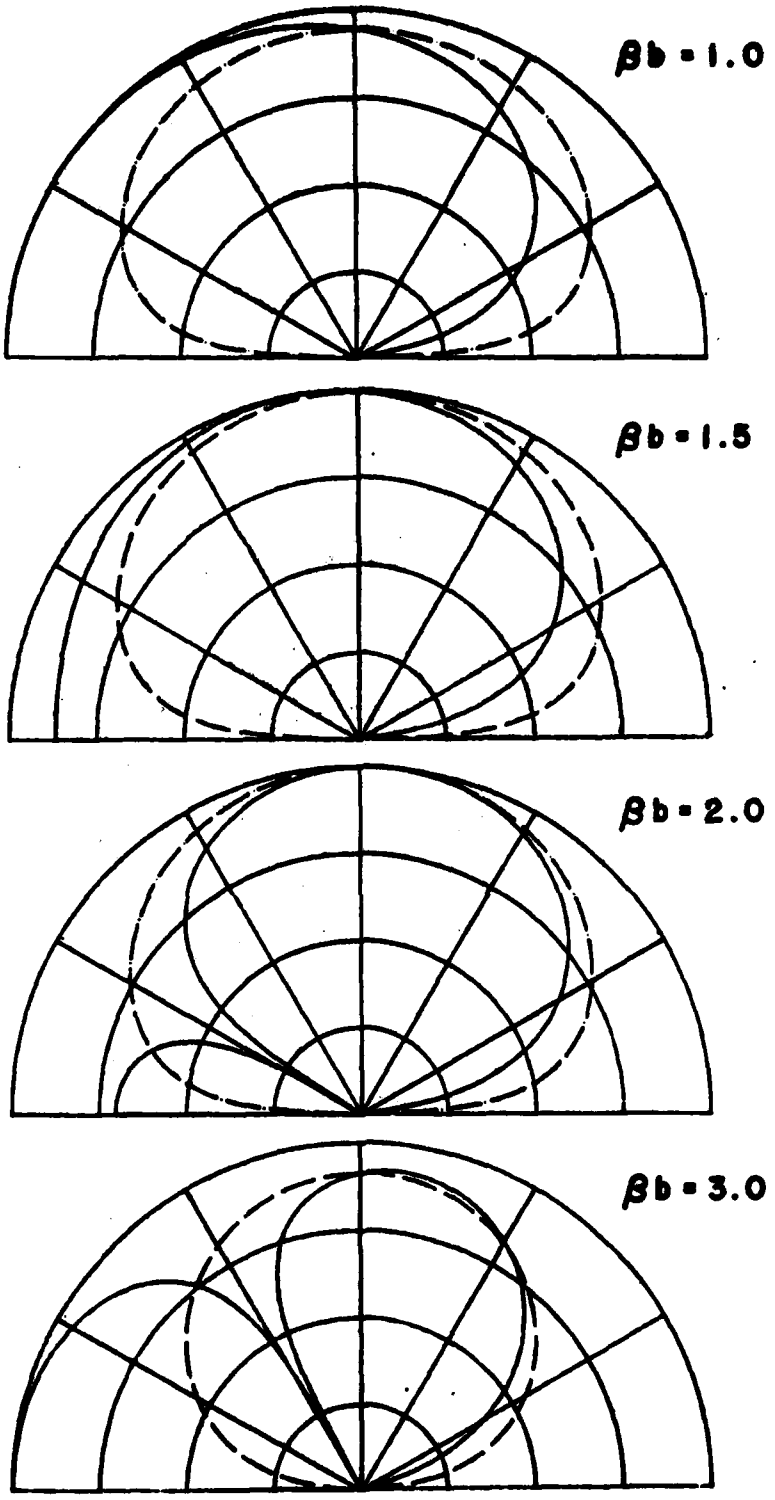

Figure 7-4. Vertical pattern at ϕ=0.

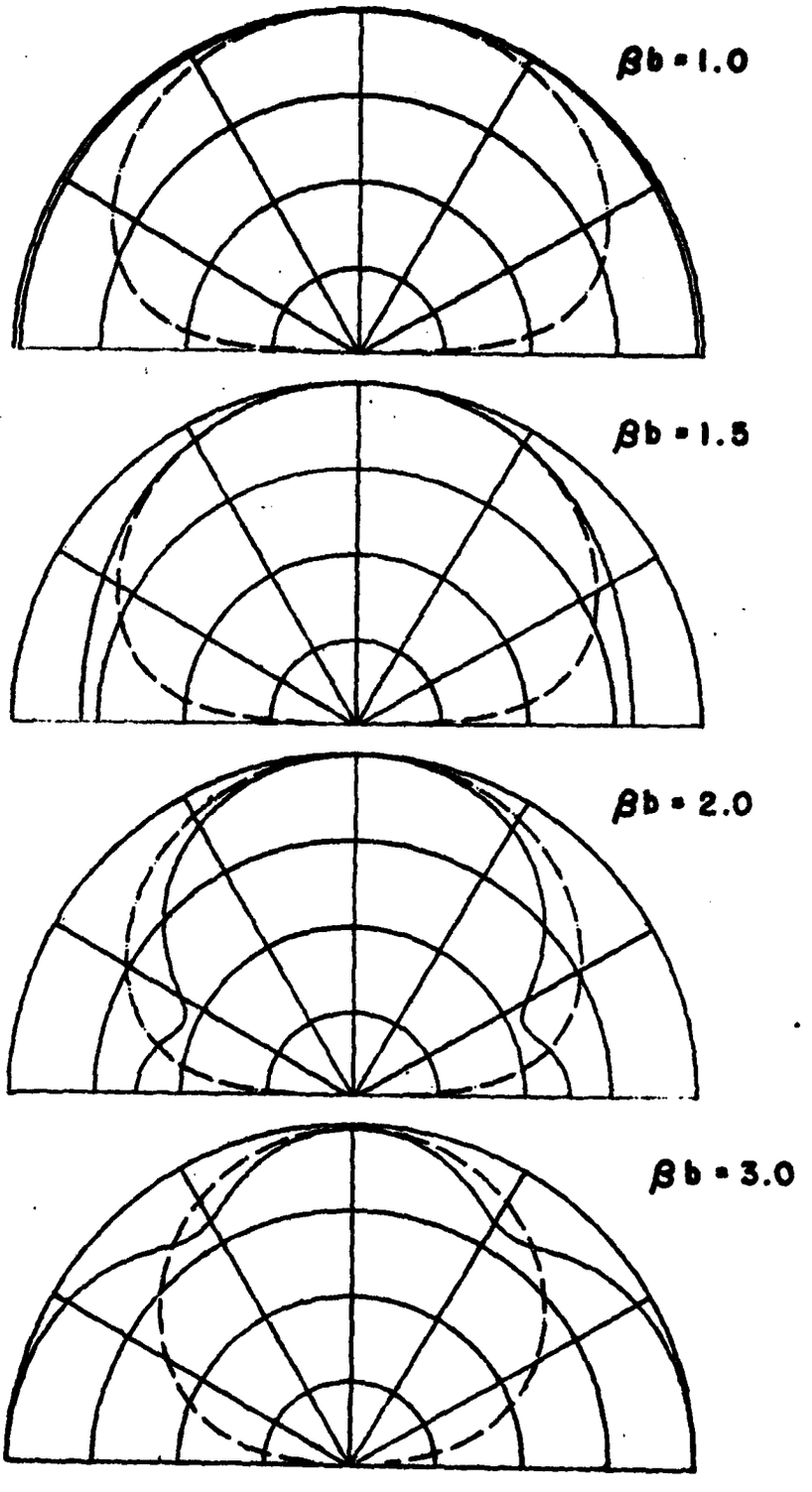

Figure 7-5. Vertical pattern at $\phi=90^{0}$.

pattern with null in 30^0 is shown. If only the amplitude ratio A is changed, the pattern is

$$E_\phi(\pi/2,\phi) \sim 1 + Ae^{i\phi} \quad . \tag{7-14}$$

This pattern is shown in Figure 7-6; A only affects the depth of null. If both amplitude and phase is changed, the pattern is a combination of Figure 7-3 and Figure 7-6. That is, the null position rotates δ and the null depth gets worse.

7.3 Comparison between the two-point-drive and four-point-drive

In this section comparison is made between the two-point-drive and the four-point-drive (both in dual loop). First, compare the horizontal pattern in Figure 3-1 (2-point-drive) with Figure 7-3 (four-pointdrive). The null width of four-point-drive is narrower than two-point-dirve. Compared with -20 dB level, two-point-drive has null of more than 70 degrees while four-point-drive has only 25 degrees. When the feeding condition is changed, each antenna behaves differently. Four-point-drive antenna changes its null direction proportional to phase difference and the null depth with the voltage ratio. However, the two-point-drive antenna changes the pattern according to both phase and amplitude ratio. The null direction remains the same.

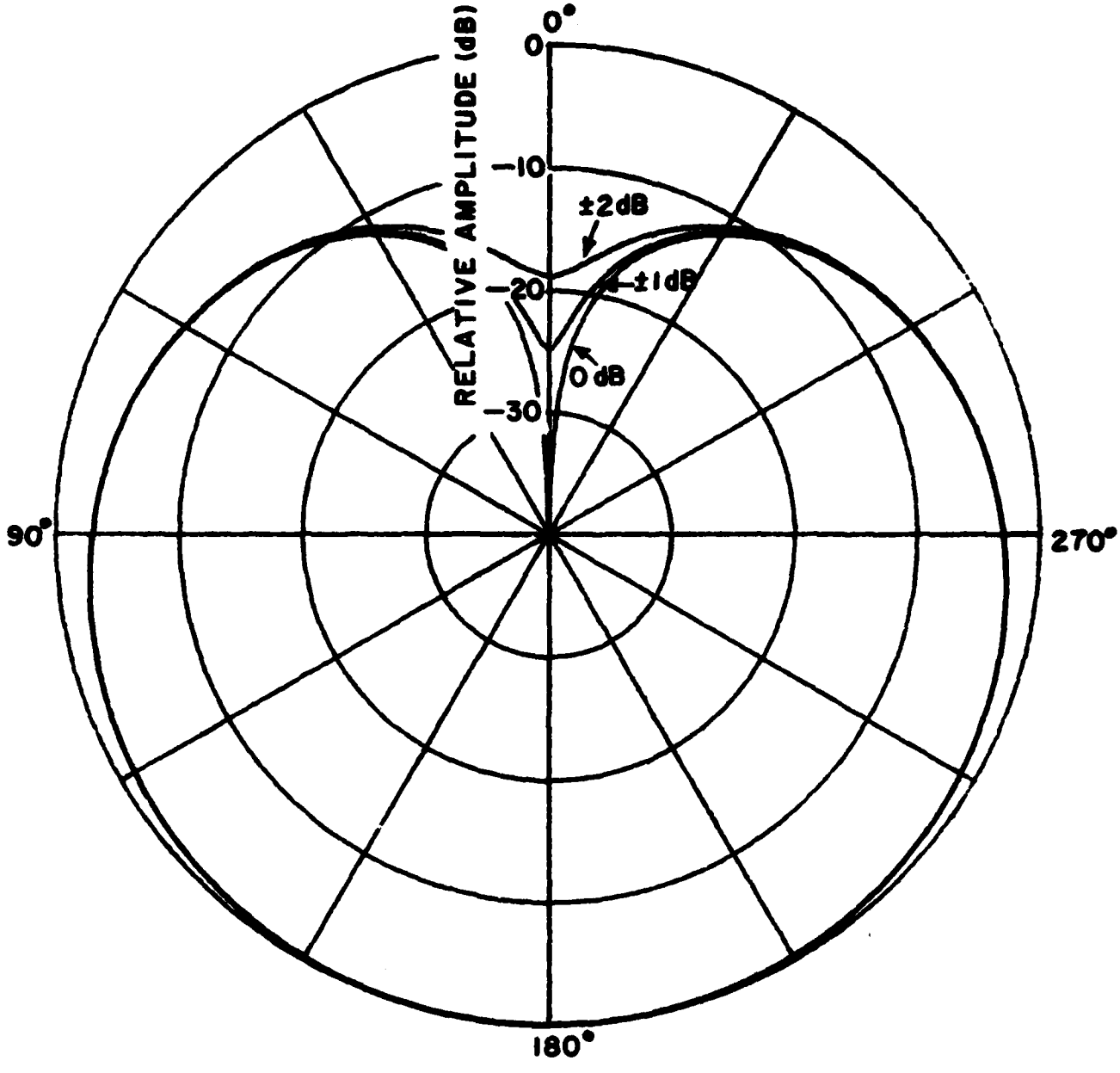

Figure 7-6. Pattern change.
Amplitude change 0, -1, -2 dB.

8. THREE POINT NULL IN SINGLE LOOP

If the n=2 mode is considered in addition to the n=0 and n=1 mode, another type of pattern can be obtained. It is possible for the pattern to have three nulls in arbitrary directions in the horizontal plane. Such an antenna is shown in Figure 8-1. The electromagnetic field is obtained by extending the method given in Section 2.3. From (2-56), $E_\theta(\pi/2, \phi)$ in the horizontal plane is

$$E_\theta(\pi/2, \phi) = 0 \ . \tag{8-1}$$

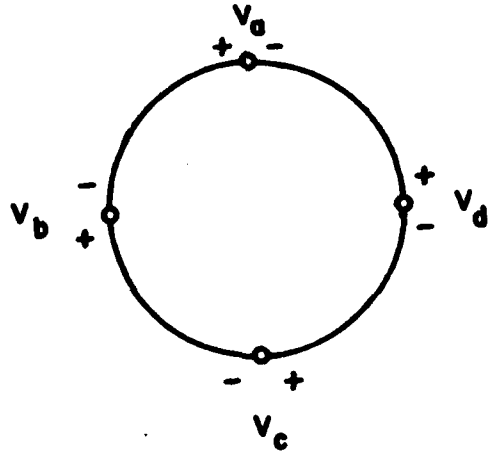

Figure 8-1. Loop antenna fed at four points.

From (2-53), we see that $E_\phi(\pi/2, \phi)$ in the horizontal plane is the sum of four voltage contributions:

$$E_\phi(\pi/2, \phi) = \omega Q V_a b \left[\frac{J_0'(\beta b)}{\alpha_0} + j \frac{2J_1'(\beta b)\cos\phi}{\alpha_1} - \frac{2J_2'(\beta b)\cos 2\phi)}{\alpha_2} \right]$$

$$+ \omega Q V_b b \left[\frac{J_0'(\beta b)}{\alpha_0} + j \frac{2J_1'(\beta b)\cos(\phi + \pi/2)}{\alpha_1} - \frac{2J_2'(\beta b)\cos 2(\phi + \pi/2)}{\alpha_2} \right]$$

$$+ \omega Q V_c b\left[\frac{J_0'(\beta b)}{\alpha_0} + j\,\frac{2J_1'(\beta b)\cos(\phi+\pi)}{\alpha_1} - \frac{2J_2'(\beta b)\cos 2(\phi+\pi)}{\alpha_2}\right]$$

$$+ \omega Q V_d b\left[\frac{J_0'(\beta b)}{\alpha_0} + j\,\frac{2J_1'(\beta b)\cos(\phi+3\pi/2)}{\alpha_1} - \frac{2J_2'(\beta b)\cos 2(\phi+3\pi/2)}{\alpha_2}\right]$$

$$= \frac{\omega Q b J_0'(\beta b)}{\alpha_0}(V_a+V_b+V_c+V_d)$$

$$+ j\,\frac{2\omega Q b J_1'(\beta b)}{\alpha_1}(V_a\cos\phi - V_b\sin\phi - V_c\cos\phi + V_d\sin\phi)$$

$$- \frac{2\omega Q b J_2'(\beta b)}{\alpha_2}(V_a - V_b + V_c - V_d)\cos 2\phi \qquad (8\text{-}2)$$

or

$$E_\phi\left(\frac{\pi}{2},\phi\right) = C_0\left[1 + C_1\,\frac{\cos\phi\,V_B\sin\phi - V_C\cos\phi\,V_D\sin\phi}{1+V_B+V_C+V_D} - C_2\,\frac{1-V_B+V_C-V_D}{1+V_B+V_C+V_D}\cos 2\phi\right] \qquad (8\text{-}3)$$

where

$$C_0 = \frac{\omega Q b J_0'(\beta b)}{\alpha_0}(V_a+V_b+V_c+V_d) \qquad (8\text{-}4)$$

$$C_1 = j\,\frac{2J_1'(\beta b)}{J_0'(\beta b)}\,\frac{\alpha_0}{\alpha_1} \qquad (8\text{-}5)$$

$$C_2 = \frac{2J_2'(\beta b)}{J_0'(\beta b)} \frac{\alpha_0}{\alpha_2} \tag{8-6}$$

$$V_B = V_b/V_a \tag{8-7}$$

$$V_C = V_c/V_a \tag{8-8}$$

$$V_D = V_d/V_a \tag{8-9}$$

In order to produce a null in the directions $\phi=\pi/2, \pi, 3\pi/2$, we require

$$E_\phi(\pi/2, \pi/2) = 0 \tag{8-10}$$

$$E_\phi(\pi/2, \pi) = 0 \tag{8-11}$$

$$E_\phi(\pi/2, 3\pi/2) = 0 \tag{8-12}$$

Solving these three equations yields:

$$V_B = V_D = \frac{C_1 + C_1C_2}{4C_2 - C_1 + C_1C_2} \tag{8-13}$$

$$V_C = \frac{-4C_2 - C_1 + C_1C_2}{4C_2 - C_1 + C_1C_2} \tag{8-14}$$

Substituting Equations (8-13) and (8-14) into (8-3) yields:

$$E_\phi(\pi/2, \phi) = C_0(1 + 2\cos\phi + \cos 2\phi) \quad . \tag{8-15}$$

This pattern is shown in Figure 8-2.

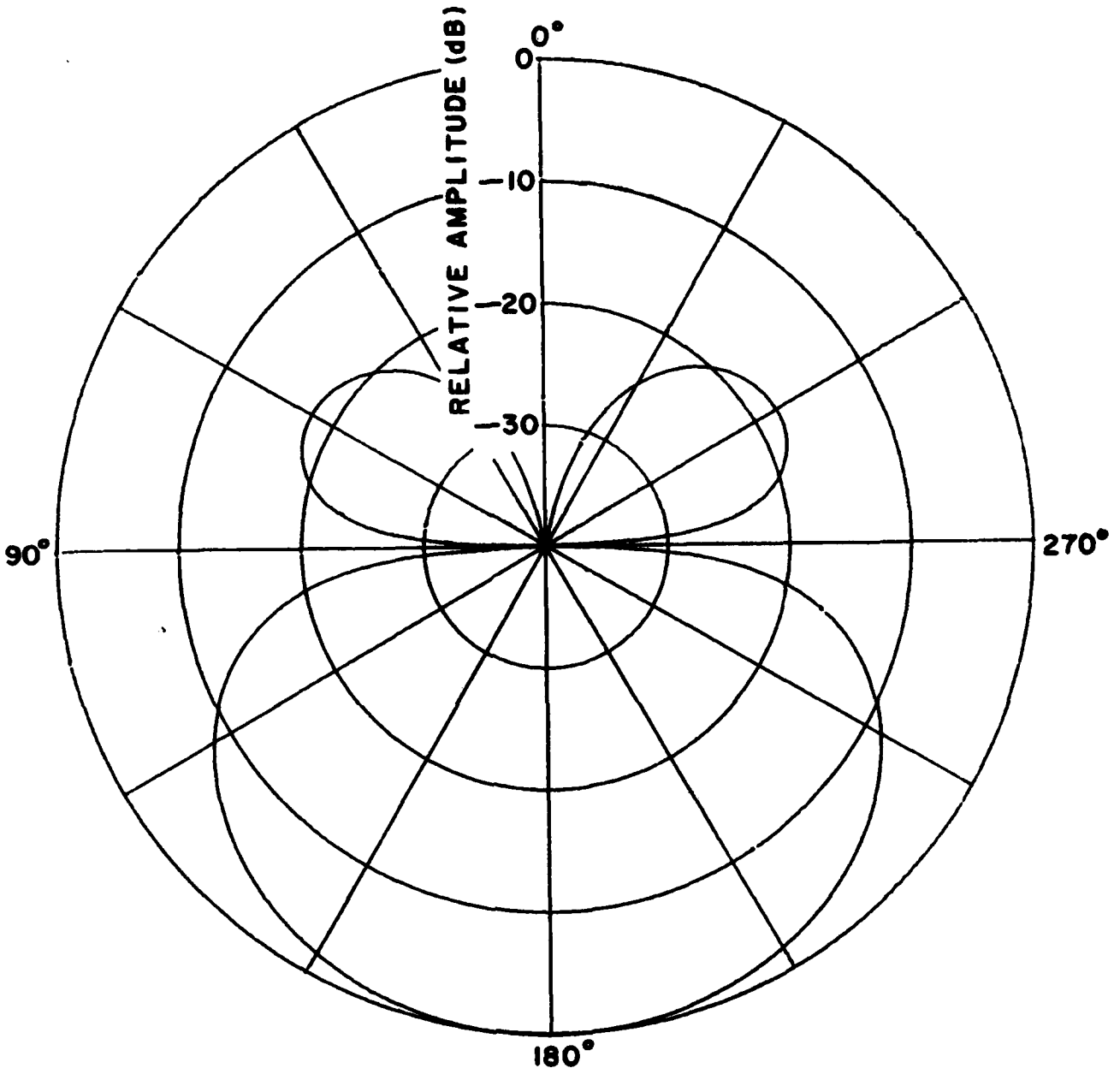

Figure 8-2. Horizontal pattern of 3-point-null.

9. THREE POINT NULL IN DUAL LOOP

Another way to obtain the three-point-null is to use dual loops as shown in Figure 9-1. The outer loop radiates only the n=2 mode. The inner loop radiates the n=0 and n=1 modes. Combination with radiation from the outer and inner loops creates the same effect as found in the previous section. Occasionally it is desirable to switch the null direction. This antenna can switch the null direction by changing only the inner loop voltage. This makes the design simpler compared with that of previous sections.

Firstly the way to obtain only the n=2 mode in the outer loop is described. General expression for $E_\phi(\pi/2,\phi)$ in four-point-drive is given by Equation (8-2). If

$$V_b=-V_a,\ V_c=V_a \text{ and } V_d=-V_a, \text{ then} \tag{9-1}$$

$$E_\phi(\pi/2,\phi) = \frac{8\omega Qb J_2'(\beta b)}{\alpha_2} V_a \cos 2\phi. \tag{9-2}$$

Therefore (9-1) is the condition for eliminating the n=0 and n=1 modes. The E-field $E_\phi(\pi/2,\phi)$ from the antenna shown in Figure 9-1 is obtained by adding (9-2) and (2-69). That is

$$E_\phi(\pi/2,\phi) = \frac{Q\omega b_{in} J_o'(\beta b_{in})(V_a+V_b)}{\alpha_o(in)}$$

$$+ j\,\frac{2\omega Q b_{in} J_1'(\beta b_{in})(V_a-V_b)\cos\phi}{\alpha_1(in)}$$

$$+ \frac{8\omega Q b_{out} J_2'(\beta b_{out}) V_c \cos 2\phi}{\alpha_2(out)} \qquad (9\text{-}3)$$

or

$$E_\phi(\tfrac{\pi}{2},\phi) = C_o\left(1 + C_1 \frac{V_a - V_b}{V_a + V_b}\cos\phi + C_2 \frac{V_c}{V_a + V_b}\cos 2\phi\right) \qquad (9\text{-}4)$$

where

$$C_o = \frac{Q\omega b_{in} J_o'(\beta b_{in})(V_a - V_b)}{\alpha_o(in)} \qquad (9\text{-}5)$$

$$C_1 = j\frac{2\alpha_o(in)}{\alpha_1(in)} \frac{J_1(\beta b_{in})}{J_o'(\beta b_{in})} \qquad (9\text{-}6)$$

$$C_2 = \frac{8b_{out}}{b_{in}} \frac{\alpha_o(in)}{\alpha_2(out)} \frac{J_2'(\beta b_{out})}{J_o'(\beta b_{in})} \qquad (9\text{-}7)$$

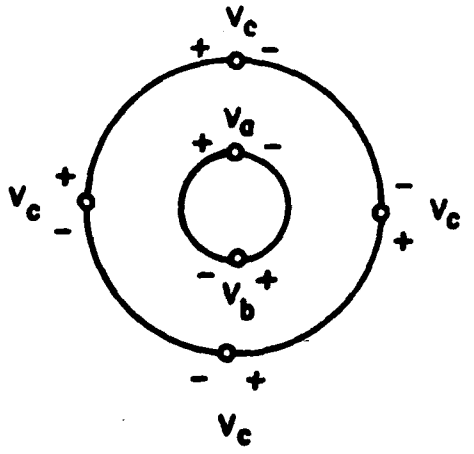

Figure 9-1. Two-loop antenna fed at four points to get 3-point null.

To obtain null at $\phi = \pi/2,\ \pi,\ 3\pi/2$ we require

$$E_\phi(\pi/2,\pi/2) = C_o\left[1 - \frac{V_c}{V_a+V_b}\,C_2\right] = 0 \qquad (9\text{-}8)$$

$$E_\phi(\pi/2,\pi) = C_o\left[1 - \frac{V_a-V_b}{V_a+V_b}\,C_1 + \frac{V_c}{V_a+V_b}\,C_2\right] = 0 \qquad (9\text{-}9)$$

$$E_\phi(\pi/2,3\pi/2) = C_o\left[1 - \frac{V_c}{V_a+V_b}\,C_2\right] = 0 \qquad (9\text{-}10)$$

That is

$$V_b/V_a = \frac{C_1-2}{C_1+2} \qquad (9\text{-}11)$$

$$V_c/V_a = \frac{2C_1}{C_2(C_1+2)} \quad . \qquad (9\text{-}12)$$

Equation (9-11) and Equation (9-12) are substituted into (9-4):

$$E_\phi(\pi/2,\phi) = C_o(1+2\cos\phi+\cos 2\phi) \qquad (9\text{-}13)$$

This is the same expression as Equation (8-15).

In an arbitrary direction we thus obtain

$$E_\phi(\theta,\phi) = j\omega Q_{in} b_{in} J_o'(\beta b_{in}\sin\theta) V_a (1+V_B)/\alpha_{in}(o)$$

$$\left[1 + j\,2\,\frac{\alpha_{in(o)}}{\alpha_{in(1)}}\,\frac{J_1(\beta b_{in}\sin\theta)}{J_o'(\beta b_{in}\sin\theta)}\,\frac{1-V_B}{1+V_B}\cos\phi\right.$$

$$\left. + 8\,\frac{b_{out}}{b_{in}}\,\frac{\alpha_{in(o)}}{\alpha_{out(2)}}\,\frac{J_2'(\beta b_{out}\sin\theta)}{J_o'(\beta b_{in}\sin\theta)}\,\frac{V_C}{1+V_B}\cos 2\phi\right] \qquad (9\text{-}14)$$

$$E_\theta(\theta,\phi) = j2\ Q\ \frac{J_1(\beta b_{in}\sin\theta)}{\alpha_{in}(1)\beta\sin\theta}\ \cos\theta\ \sin\phi\ (V_a - V_b)$$

$$- j16\ \frac{Qb_{out}}{\alpha_{out}(2)}\ \frac{J_2(\beta b_{out}\sin\theta)}{\beta b_{out}\sin\theta}\ \cos\theta\ \sin 2\phi\ V_c \qquad (9\text{-}15)$$

The vertical patterns at $\phi=0$ and $\theta=90^0$ are shown in Figure 9-2 and 9-3, respectively. Figures 9-4 and 9-5 show the change of the pattern when the feeding condition is changed. Figure 9-4 shows the change as a function of $V_B = V_b/V_a$ (that is voltage and phase of the small inner loop) while Figure 9-5 shows the change as a function of $V_C = V_c/V_a$ (that is those of the outer loop are changed).

10. CONCLUSION

The radiation pattern of a single loop and two concentric loops fed at one, two or four points were investigated. It was found that a single loop is capable of producing two nulls which can be made to coincide and produce a true cardoid pattern. Three nulls could also be produced by feeding a single loop at four points or by one of two concentric loops. Particular attention was given to the tolerances to be imposed on the feeding voltages to maintain a reasonable null level. It is concluded that to obtain a large bandwidth (>10%), some compensation should take place in the feeding network. This is illustrated in another report [2] when an annular slot antenna fed at four points and with a flush mounted monopole in the middle has been developed and yields a bandwidth of 25% with an FB-ratio of more than 15 dB.

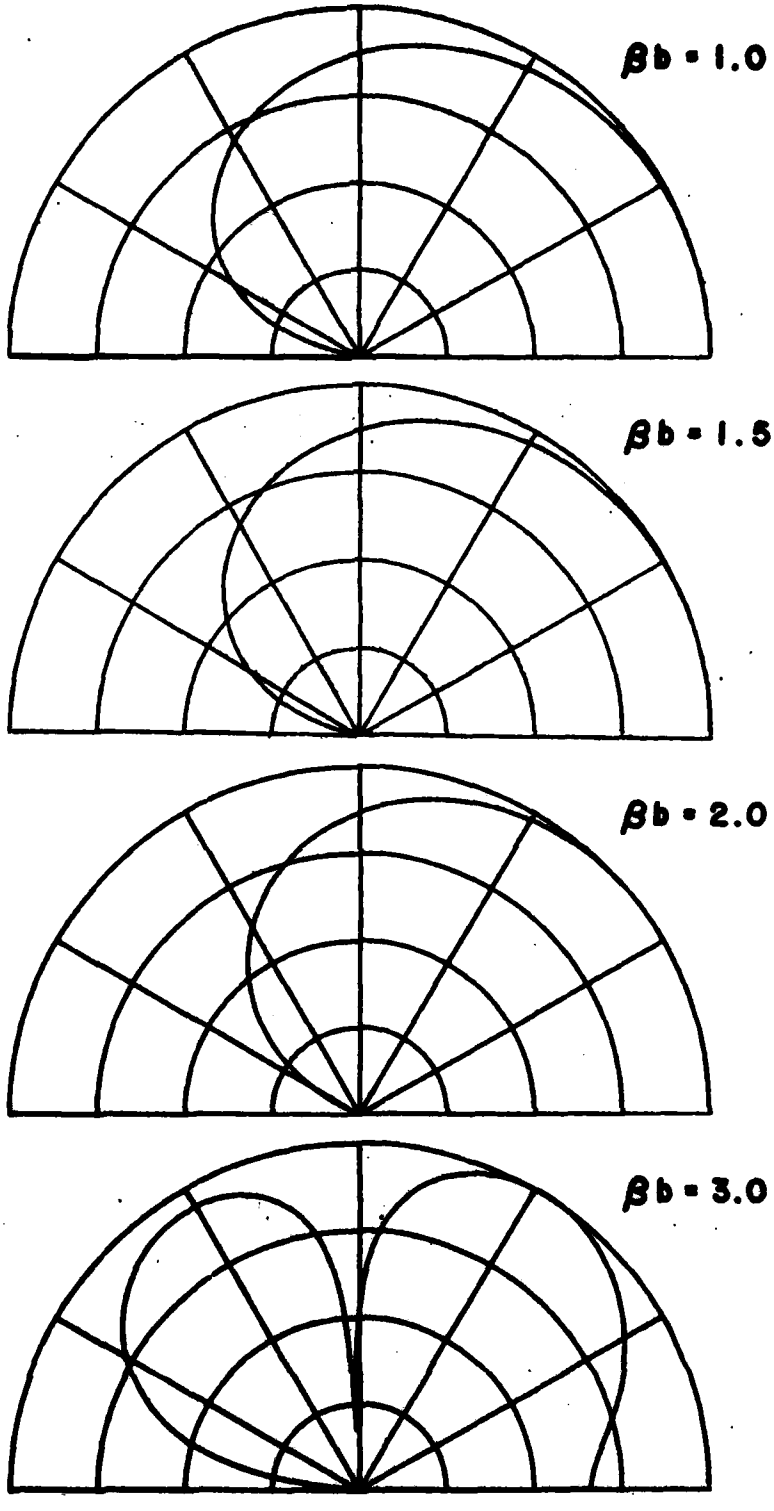

Figure 9-2. Vertical pattern at $\phi=0^{0}$.

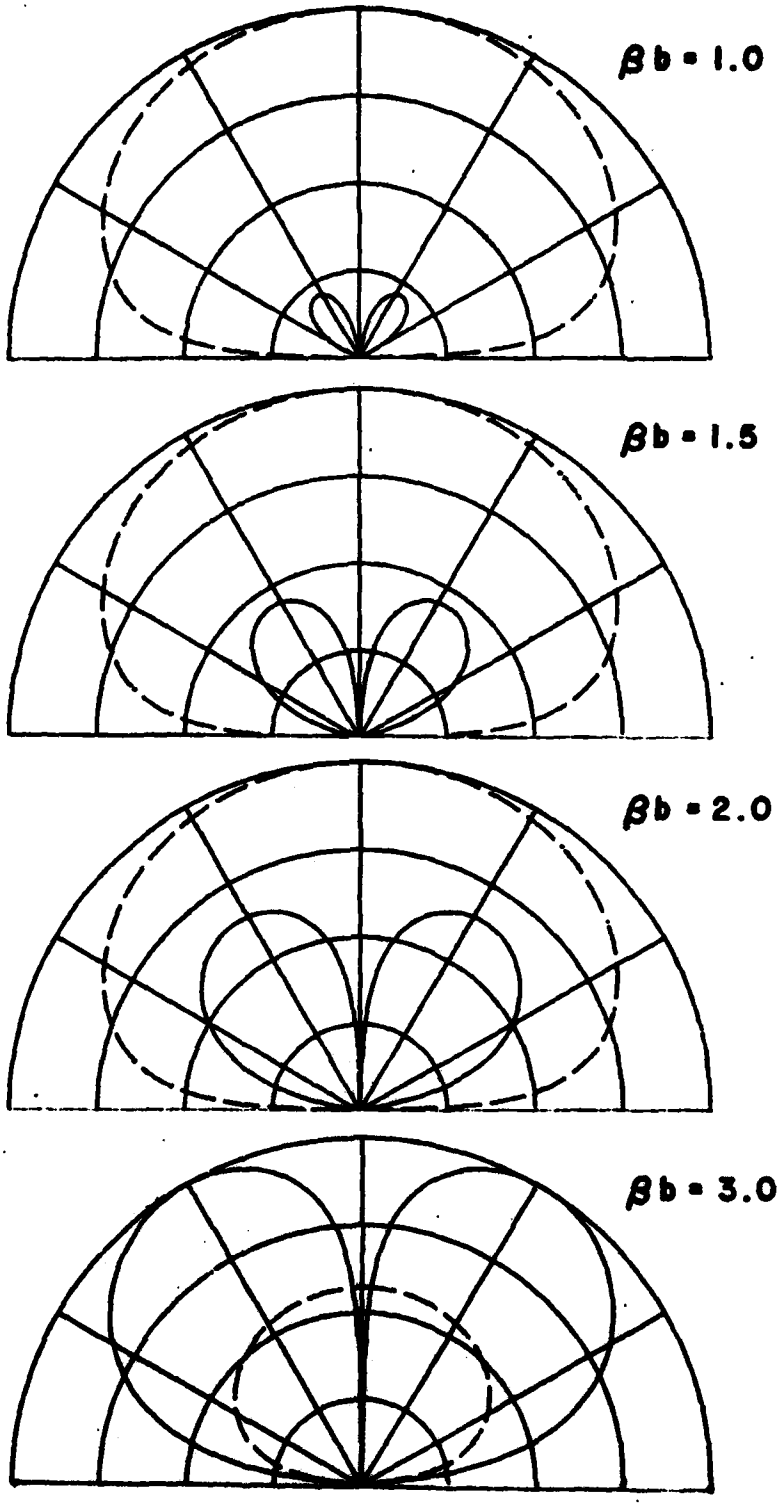

Figure 9-3. Vertical patterns at $\phi=90^{\circ}$.

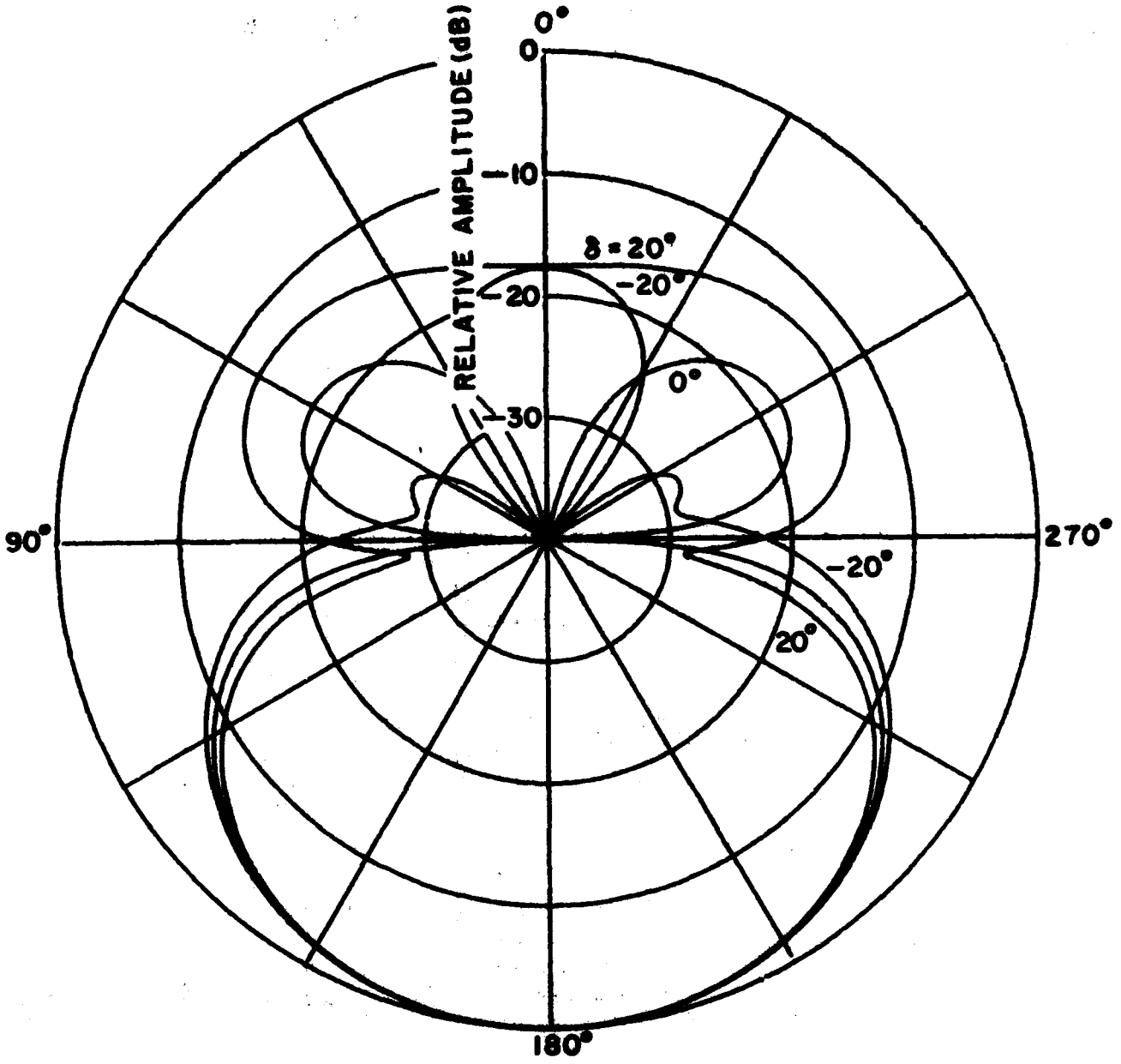

Figure 9-4(a). Pattern change.
Phase of inner loop changed.

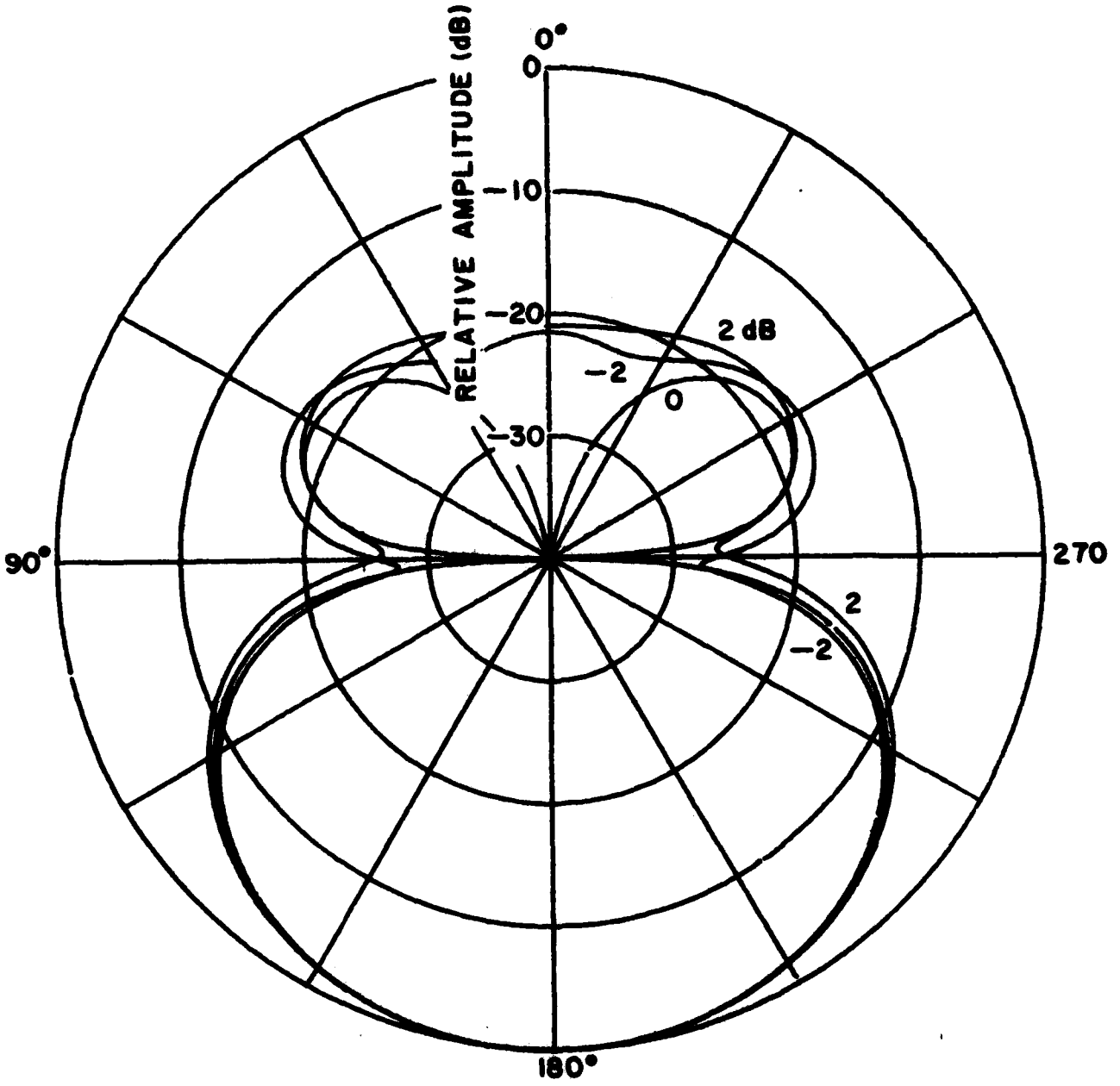

Figure 9-4(b). Pattern change.
Amplitude of inner loop changed.

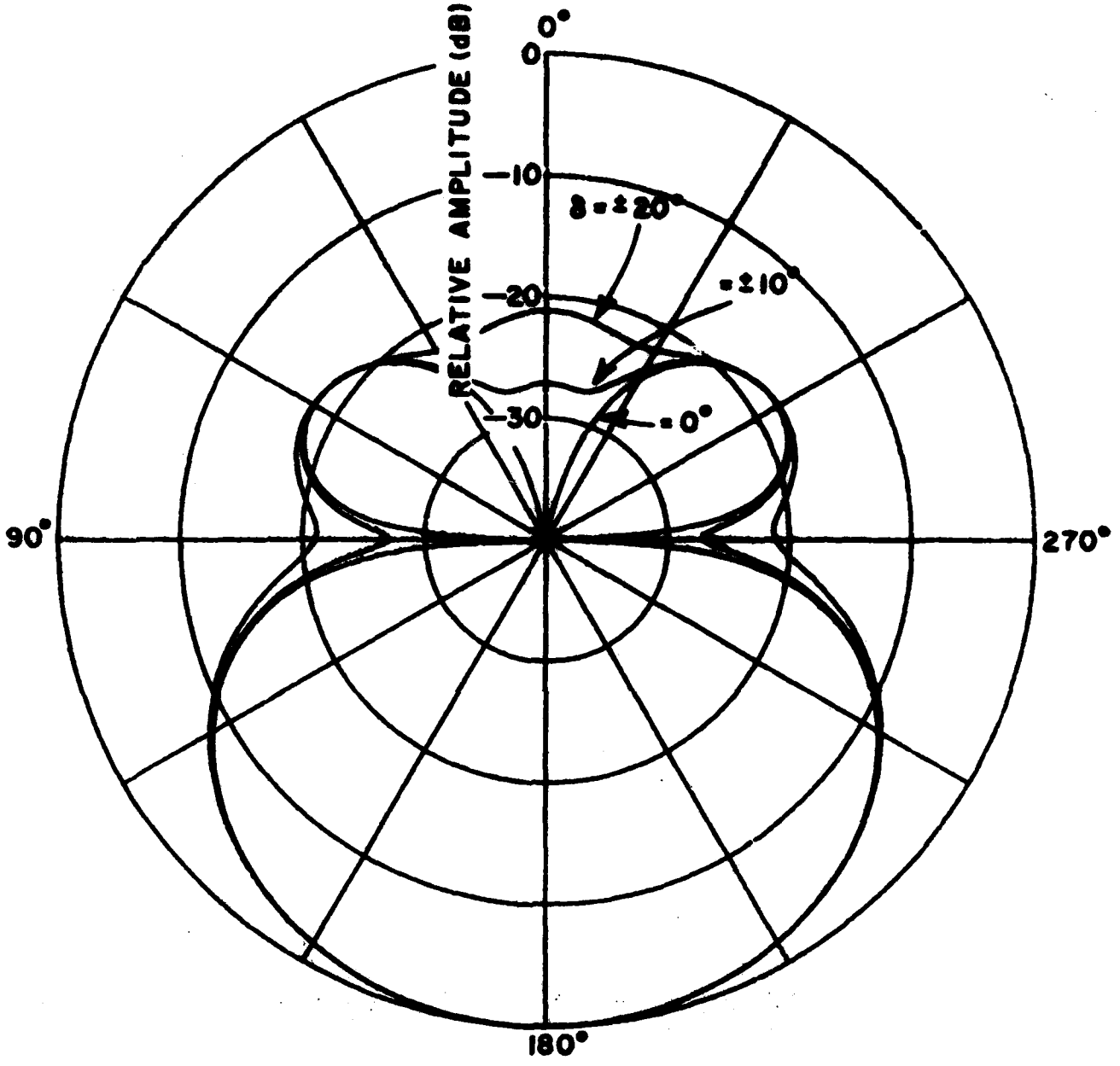

Figure 9-5(a). Pattern change.
Phase of outer loop changed.

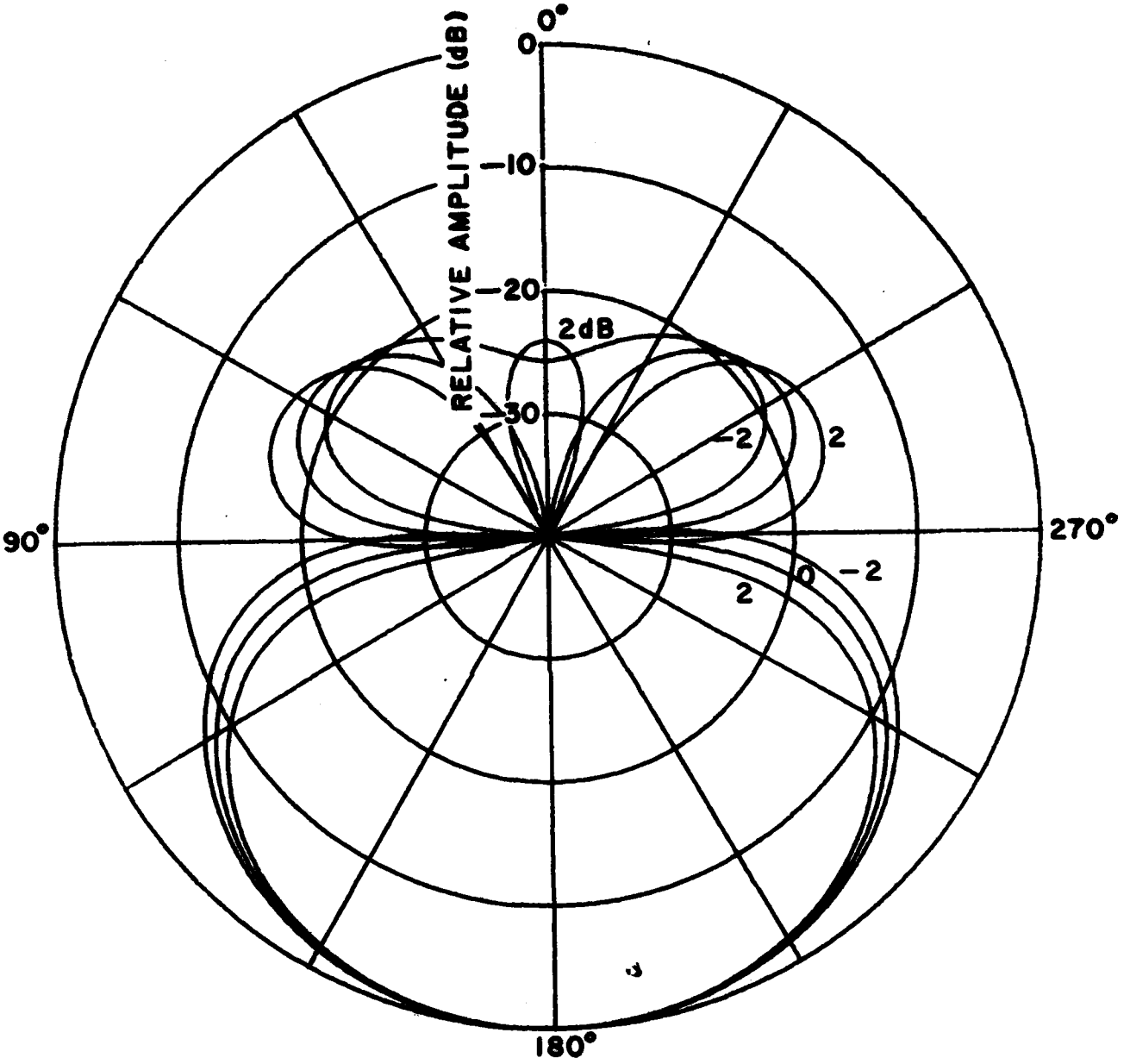

Figure 9-5(b). Pattern change.
Amplitude of outer loop changed.

REFERENCES

1. R.W.P. King and C.W. Harrison, Jr., Antennas and Waves, A Modern Approach, MIT Press, 1969, Chapter 9.

2. B. A. Munk and C. J. Larson, "A Cavity-Type Broadband Antenna with a Steerable Cardioid Pattern," Final Report 711559-2, December 1979, The Ohio State University ElectroScience Laboratory, Department of Electrical Engineering; prepared under Contract N00014-78-C-0855 for Office of Naval Research.